Spring 1985

KINETIC, SPECTROSCOPIC AND CHEMICAL MODIFICATION STUDY OF IRON RELEASE FROM TRANSFERRIN; IRON(III) COMPLEXATION TO ADENOSINE TRIPHOSPHATE (ETHOXYFORMIC ANHYDRIDE, LYSINE)

CARL PERLEY THOMPSON
University of New Hampshire, Durham

Thompson, Carl Perley

KINETIC, SPECTROSCOPIC AND CHEMICAL MODIFICATION STUDY OF IRON RELEASE FROM TRANSFERRIN; IRON(III) COMPLEXATION TO ADENOSINE TRIPHOSPHATE

University of New Hampshire PH.D. 1985

KINETIC, SPECTROSCOPIC AND CHEMICAL MODIFICATION STUDY OF IRON RELEASE FROM TRANSFERRIN; IRON(III) COMPLEXATION TO ADENOSINE TRIPHOSPHATE

BY

CARL P. THOMPSON
BA, University of Maine at Orono, 1978

A DISSERTATION

Submitted to the University of New Hampshire
in Partial Fulfillment of
the Requirements for the Degree of

Doctor of Philosophy
in
Chemistry

May, 1985

This dissertation has been examined and approved.

N. Dennis Chasteen

Dissertation director, N. Dennis Chasteen
Professor of Chemistry

Paul R. Jones

Paul R. Jones, Professor of Chemistry

Thomas M. Laue

Thomas M. Laue, Assistant Professor of Biochemistry

Rudolf Seitz

Rudolf W. Seitz, Professor of Chemistry

Edward H. S. Wong

Edward Hou S. Wong, Associate Professor of Chemistry

March 18, 1985

Date

ACKNOWLEDGEMENTS

I have been fortunate enough to be associated with many fine people through the years. It is to them that I owe a debt of gratitude. Drs. Amell, Seitz, Weber and Wong were among my first contacts at UNH, and it is partly because of their encouragement that I pursued a graduate program in Chemistry. Many students who have since departed, but remain good friends include Dave Ryan, Joe Ciejka, Paul Rosenberg, Bill Orem, Don Folajtar, Manny Almeida, Jamie Rines and Ellen Lord. These friends helped to forge the way and made life much easier for me.

One of the smartest moves that I made at UNH was to enter the Chasteen Research Group. The program that Dr. Chasteen has undertaken is an ambitious one and the opportunity to participate in stimulating scientific research proved to be excellent.

Because of my association with Dr. Chasteen, I have been able to interact with many distinguished visitors, such as Dr. George Bates (Texas A & M), Dr. Elizabeth Theil (North Carolina State University), Prof. Pauline Harrison (The University of Sheffield), Dr. Clive Hollaway (York University), Dr. Jeff Wardeska (East Tennessee State), Dr. Robert Woodworth (University of Vermont College of Medicine), and Dr. Thomas Gill. Other distinguished personnel in the Chasteen group include Donna Martin, Barbara Viglione, Sue Swope and John Grady. Dr. Chasteen's high standards of professionalism, research quality and scientific integrity have been inspiring over the years. If a portion

of his influence rubs off on me, then I am certain that my future scientific endeavors will be successful.

Laboratory assistance from Barbara McCarty, Cindy Burns and John Grady is much appreciated. Also I would like to extend my thanks to Ms. Eileen Wong, who typed the thesis and provided other technical assistance in the preparation of this thesis. The work was generously supported by NIH Grant GM20194-10,-11, and -12.

I would like to express my sincere appreciation to my Dad, Mr. Perley Thompson, my Mom, the late Mrs. Sarah Thompson, and Peggy's folks, Don and Kitty Ross. And finally, to Peggy and Benjamin, but especially to my wife Peggy, whose love, hardwork and personal sacrifice throughout my graduate school days have never been taken for granted. It is to her that I dedicate this thesis.

TABLE OF CONTENTS

LIST OF FIGURES

LIST OF TABLES

ABSTRACT

KINETIC, SPECTROSCOPIC AND CHEMICAL MODIFICATION STUDY OF IRON RELEASE FROM TRANSFERRIN; IRON(III) COMPLEXATION TO ADENOSINE TRIPHOSPHATE

by

Carl P. Thompson
University of New Hampshire, May, 1985

Amino acids other than those that serve as ligands have been found to influence the chemical properties of transferrin iron. The catalytic ability of pyrophosphate to mediate transferrin iron release to a terminal acceptor is largely quenched by modification of non-liganded histidine groups on the protein. The first order rate constants of iron release for several partially histidine modified protein samples were measured. A statistical method was employed to establish that one non-liganded histidine per metal binding domain was responsible for the reduction in rate constant. These results imply that the iron mediating chelator, pyrophosphate, binds directly to a histidine residue on the protein during the iron release process. EPR spectroscopic results are consistent with this interpretation. Kinetic and amino acid sequence studies of ovotransferrin and lactoferrin, in addition to human serum transferrin, have allowed the tentative assignment of His-207 in the N-terminal domain and His-535 in the C-terminal domain as the groups responsible for the reduction in rate of iron release.

The above concepts have been extended to lysine modified transferrin. Perchlorate induces changes in the EPR spectra and kinetics of iron release in human serum transferrin; similar effects

are also induced by lysine modification and found to occur primarily in the C-terminal domain. Furthermore, the labilizing effect of 0.5 M sodium perchlorate on iron in the C-terminal site is largely quenched by lysine modification. The above experiments suggest that the well studied "perchlorate effects" in transferrin are caused by anion binding at a small number (< 15) of lysines, probably located close to the metal.

Complexation of iron(III) to adenosine triphosphate (ATP) was also studied to gain insight into the nature of iron-ATP species present at physiological pH. At pH 7.0, mononuclear (metal:ligand <1:3) and polynuclear (metal:ligand = 2:1 and 4:1) readily form in solution. The mononuclear complexes exhibit a $g' = 4.3$ EPR signal. ^{31}P NMR spectra are observed when ATP is present in large excess. The polynuclear (4:1 metal:ligand) complex, although polydisperse in size, has a molecular weight greater than 50,000, indicating cluster formation (< 250 iron atoms per cluster). These complexes are EPR silent and give no ^{31}P NMR spectra consistent with findings for other reported polynuclear iron(III) complexes.

INTRODUCTION

The importance of iron as an essential trace metal has long been recognized (1). The well studied iron containing respiratory proteins, hemoglobin and myoglobin, account for about three-fourths of the body iron stores (1,2). Heme proteins are biosynthesized in the hemopoietic tissues: liver, spleen, and bone marrow. To meet the requirements of hemopoiesis, iron is constantly being mobilized from two sources, diet and iron storage. A great deal is known about the metabolism of iron, but the details of iron transfer within the cell remain the focus of much current research.

Under physiological conditions of pH and oxygen tension, free iron in the absence of chelators is known to hydrolyze and form insoluble polymers that precipitate from solution. Because of these inherent chemical problems, nature has evolved an intricate system of proteins and anions that ensures solubilization and facile mobilization of body iron. The major form of dietary iron, which is absorbed from the intestine, is iron(II). Once in the bloodstream, following oxidation, the iron(III) form is bound tightly by serum transferrin, which sequesters and stabilizes the iron. Transferrin transports the metal to the iron storage protein, ferritin. Nearly twenty-five percent of all body iron is associated with ferritin.

Transferrins

The transferrins are an important class of metal binding proteins found widely in nature (3,7). In egg whites, as ovotransferrin, and in milk, as lactoferrin, the protein acts as

a bacteriostatic agent, denying bacteria nutritional iron sources. The transferrins are β-globulins consisting of a single polypeptide chain of approximately 80,000 molecular weight. As with other transferrins, human serum transferrin is a two-sited protein, binding two metals in separate domains of the protein, generally referred to as C- and N-terminal sites.

The metal binding sites appear to be nearly structurally equivalent. Chemical modification studies provide some insight into the identity of the ligands of the iron binding sites. Nitration suggests three tyrosines per metal site (8). Other methods indicate two (9). Ethoxyformylation and photooxidation experiments implicate two histidines per iron (10,11). Phenylglyoxallation (12) suggests one arginine. Lysines have been ruled out as possible ligands since iron binding is not affected by acetylation (13).

The amino acid sequences for human serum transferrin (14) and ovotransferrin (15) reveal large degrees of homology between their respective C- and N-terminal domains. It is currently believed that transferrin evolved from an ancestral single-sited protein of about 40,000 molecular weight (16). Ancestral gene duplication is one theory that explains the doubling in molecular size and thus the observed homology between the two domains of the protein.

Transferrin possesses a remarkable affinity for iron under physiological conditions, having an effective binding constant of 10^{24} M^{-1} (17). Yet due to nutritional demands, transferrin effectively and efficiently turns over its iron about ten times in a 24 hour period (18,19). The source of the thermodynamic stability but kinetic lability of the iron-transferrin complex remains a perplexing question.

Transferrin-anion Interactions

The biological significance of anion participation in iron metabolism has received increased attention from investigators in recent years. In 1976, Bartlett found significant amounts of iron associated with adenosine triphosphate (ATP) in the cytosol of human red blood cells (20). He also showed that 1:1 iron-ATP complexes were stable under physiological conditions. In 1981, Crichton reported an *in vitro* study demonstrating the direct iron transfer from transferrin to ferritin, mediated by ATP (21). Due to the high stability of transferrin-iron, the usual flow of iron is from ferritin to transferrin, in the absence of ATP (22).

In light of Bartlett's findings, Crichton proposed that iron-ATP complexes play an important role in intracellular iron metabolism. In blood sera and the cytosol of cells, several anions including citrate and chloride are present in significant concentrations (20). Little is known about the role of such anions, *in vivo*, but evidence is growing that the ionic composition of blood sera and the cytosol of cells plays a role in facilitating the transfer of iron from transferrin to ferritin and iron-requiring tissues.

In 1980, Williams and Moreton reported that the distribution of iron between the two sites of transferrin in equilibrated serum is changed by dialysis, whereupon iron, predominantly in the N-terminal site, is redistributed to the C-terminal site (23). Baldwin and de Sousa (24) and Williams *et al.* (25) have suggested that this change is caused by removal of the ionic components, principally NaCl, from serum. Consistent with this hypothesis is the observation that *in vitro* the presence of salt favors iron binding in the N-terminal site,

whereas the opposite is true of the C-terminal site (25). The salt effect does not appear to be simply due to a change in ionic strength, although that is probably a contributing factor, since different salts at the same ionic strength influence the distribution of iron on the protein to different degrees. The interactions of anions and cations with the protein probably induce conformational changes which in turn alter the thermodynamic stability of iron binding to the two sites. Baldwin and co-workers have discussed this subject in detail (24,26).

Chelating agents such as pyrophosphate, ATP, and citrate have been found to mediate <u>in vitro</u> the release of iron from transferrin to a terminal acceptor molecule such as desferrioximine B which has a higher affinity for Fe(III) than the protein (27,28). Recently Bates and co-workers have provided experimental evidence for the formation of a quaternary intermediate complex of the type Chel-Fe-Tf-HCO_3 in the exchange of iron between apotransferrin, Tf, and a chelating agent, Chel (29). In such a complex the chelating agent is presumably bound to the iron, but may also interact directly with the protein through cationic side chains of amino acid residues, located near to the metal.

The rate of iron removal from transferrin by chelators is changed by the presence of salt (24,25). Salt concentrations in the range of 0.1 - 1.0 M accelerate the rate of iron removal from the C-terminal site, but retard the rate from the N-terminal site. Thus salt stabilizes the N-terminal site relative to the C-terminal site, both kinetically and thermodynamically. Sodium perchlorate is the most effective sodium salt in altering the properties of the protein. The effect is believed to be largely due to the perchlorate rather than the sodium.

The presence of salt also induces changes in the EPR spectrum of transferrin. The relationship between these changes and those in the kinetic and thermodynamic properties of the protein is, however, unclear. Price and Gibson first observed that perchlorate causes a reduction in the amplitude of the g' = 4.3 Fe^{3+} signal and the appearance of a shoulder on the low field side of this signal (30). These observations were attributed to a conformational change occurring in one domain of the diferric protein. Baldwin and co-workers have examined the effect of perchlorate on the EPR spectra of the monoferric transferrins and have concluded that only the C-terminal domain undergoes a conformational change (26). Their spectrum of the C-terminal monoferric transferrin in the presence of sodium perchlorate is in accord with that previously observed in this laboratory (31).

Recently our laboratory reported that the sodium salts of various anions alter the EPR spectrum of diferric transferrin (32). Diferric transferrin solutions were titrated with various anions and the EPR difference quantitated. The binding constants and stoichiometries were derived from Hill plots. The binding constants were observed to follow the lyotropic series, i.e. $SCN^- > ClO_4^- > P_2O_7^{4-} > Cl^- > AMP^{2-}$, HPO_4^{2-}, SO_4^{2-}, F^-. The data are consistent with an anion binding phenomenon, possibly to positively charged protein groups, near to the metal.

An amino acid string model of the probable metal locus of the transferrin N-terminal domain has been recently proposed (33). The model (see Appendix) shows a number of cationic groups, i.e. several lysines, two arginines, and one histidine located near the probable metal ligands, Tyr 185, Tyr 188, His 119, and His 249. Protein folding upon iron binding may bring several of these groups in close proximity

to the metal. The richly cationic character of the metal region, due to the presence of these groups, may partly be responsible for the observed protein-anion interactions discussed above.

This dissertation research was undertaken to further delineate the roles that anions play in the metabolism of iron. In Chapter 1, the studies of the role of pyrophosphate in transferrin iron exchange reactions are presented. The involvement of a key histidine in the reaction is identified by chemical modification. Chapter 2 is dedicated to the identification of amino acid residues involved in the spectral and kinetic effects of salt on the protein, also using chemical modification. Finally, an investigation of iron-ATP complexation of potential biological significance is discussed in Chapter 3.

CHAPTER I

EFFECT OF MODIFICATION OF NON-LIGANDED HISTIDINES ON THE PYROPHOSPHATE CATALYZED IRON RELEASE REACTION OF DIFERRIC TRANSFERRIN

INTRODUCTION

It is well known that the thermodynamic stability of the iron transferrin complex is significantly reduced below pH 7.5 (17,25,31) and that the rate of iron removal by mediating chelators is greatly enhanced (27-29,34). These changes occur in the pH range where histidines normally titrate. Accordingly, a chemical modification study of the influence of non-liganded histidines on the kinetics of iron removal from transferrin was undertaken. Previous histidine modification studies by Feeney and co-workers (10) and others (11,35) have implicated four histidines as ligands, two per iron, in human serum transferrin.

The most common reagent for modifying histidine residues is ethoxyformic anhydride (EFA) (36). It hydrolyzes slowly in water to give two equivalents each of ethanol and carbon dioxide (or bicarbonate). EFA reacts principally with protein imidazole groups (eq. 1.1) and is easily quantifiable spectrophotometrically.

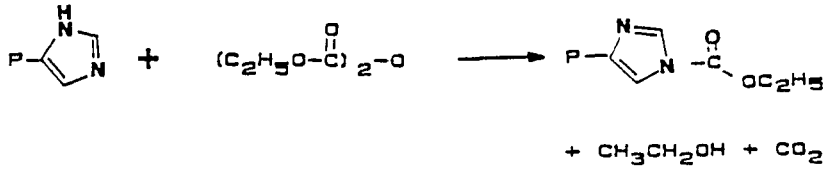

(1.1)

In the present study the ethoxyformylation reaction was used to modify the histidines of diferric transferrin to different extents followed by detailed study of the kinetics of iron removal from these modified proteins. The pseudo first-order rate constant for iron release from either site, using pyrophosphate as a mediator and desferrioximine B as an iron sink, is appreciably reduced by

modification. In addition, modification imparts considerable kinetic stability to the protein at pH 5. The data suggests that the modification of key histidines, one in each of the two iron binding domains, is responsible for these effects. These results point toward an important role for non-liganded histidine residues in iron exchange reactions of transferrin.

MATERIALS AND METHODS

Transferrin

Human serum transferrin of stated 98% purity was obtained from Cal-Biochem. Co. and used without further purification. The protein was brought to 80-90% saturation by the addition of a quantitative volume of 0.01 M ferrous ammonium sulfate in 0.01 M HCl to 0.2 mM apoprotein in 0.1 M Hepes, 0.01 M $NaHCO_3$, pH 7.5. The concentration of apotransferrin was determined spectrophotometrically using the molar absorptivity of $\varepsilon^{280nm} = 8.89 \times 10^4\ M^{-1}cm^{-1}$ (37). The percent saturation was determined using $\varepsilon^{465nm} = 2500\ M^{-1}cm^{-1}$ per bound iron (4).

C-terminal monoferric transferrin was prepared as follows: 0.17 mM apotransferrin in 0.1 M Hepes· Na/0.02 M $NaHCO_3$ at pH 7.5 was titrated past its endpoint with a 0.010 M iron(III):nitrilotriacetate (1:2), pH 4 solution. Absorbance was scanned between 450 and 470 nm using a Cary 219A recording double beam spectrophotometer. After determination of the titration endpoint, sufficient $Fe(NTA)_2$ was added to 45% saturate the protein. Excess nitrilotriacetate was removed by treatment with 0.1 M $NaClO_4$ (chelexed) and subsequent dialysis against 0.01 M NH_4HCO_3. The resulting protein was lyophilized and stored at 4°C. Purity of the monoferric preparation was determined by running urea polyacrylamide gel electrophoresis (urea-PAGE).

Ethoxyformylation

Reagent grade liquid ethoxyformic anhydride (EFA) was obtained from Aldrich Chemical Co. and used without purification or dilution.

The diferric protein at a concentration of 4.2 - 10 uM in 0.1 M Hepes·Na, 0.01 M $NaHCO_3$, pH 7.3 - 7.4 was modified by adding microliter quantities of EFA to achieve final concentrations ranging from 0.22 mM to 1.36 mM. The extent of the modification was monitored using Cary 219A or Bausch Lomb 505 spectrophotometers and the unmodified protein solution as a reference. The number of histidines modified was calculated from the molar absorptivity for the difference spectrum, i.e. $\varepsilon^{242\ nm} = 3200\ M^{-1}cm^{-1}$ per histidine monoethoxyformylated (38). Separation of the low molecular weight reaction products from the protein was achieved with a 3 ml or 50 ml Amicon ultrafiltration cell fitted with a PM 10 membrane. The volume was replaced three times (90% V/V per change) with fresh 0.1 M Hepes, 0.02 M $NaHCO_3$ buffer.

The biphasic semi-logarithmic plot of the extent of modification versus time was least squares curve fitted to equation 1.2 for two pools, A and B, of reactive histidines, i.e.

$$A_{242} = A_\infty \{1 - \underline{X}_A \exp(-\underline{k}_A t) - \underline{X}_B \exp(-\underline{k}_B t)\} \qquad (1.2)$$

where $\underline{k}_A$ and $\underline{k}_B$ are the first-order rate constants and $\underline{X}_A$ and $\underline{X}_B$ ($= 1 - \underline{X}_A$) are the corresponding mole fractions of the fast and slowly reacting pools, respectively. This equation assumes equal molar absorptivities for histidines in either pool.

Iron Removal Reactions

The kinetics of iron removal from unmodified, partially modified, and fully modified samples of 15 - 20 uM diferric transferrin in 0.1 M Hepes, 0.02 M $NaHCO_3$, pH 6.9 was carried out in a quartz cuvette at 37.0 $\pm$ 0.1°C in the thermostatted sample compartment of a Cary 219A spectrophotometer using buffer as the reference solution. A 0.100 M

solution of pyrophosphate (Sigma) and a 0.030 M solution of desferrioximine B (Ciba), both in buffer, were added to sample and reference cells to give final concentrations of 3.0 mM and 0.90 mM, respectively, unless otherwise stated. The reaction was monitored by following the decrease in absorbance at 295 nm with time.

Absorbance vs. time curves were fitted by a least squares simplex optimization procedure to equation 1.3.

$$A_{295} = (A_o - A_\infty)\{\underline{X}_1 \exp(-\underline{k}_N t) + \underline{X}_2 \exp(-\underline{k}_C t)\} + A_\infty \qquad (1.3)$$

where $\underline{k}_N$ and $\underline{k}_C$ are the pseudo-first order macroscopic rate constants for iron removal from the N- and C-terminal binding sites at, respectively. Molar absorptivity (ε) values at 295 nm of 12600 $cm^{-1}M^{-1}$ and 14040 $cm^{-1}M^{-1}$ were determined for the C and N sites, respectively. $\underline{X}_1$ and $\underline{X}_2$ in eq. 1.3 are weighting coefficients calculated as follows: $\underline{X}_1 = \underline{X}_N \dfrac{\varepsilon_N}{(\varepsilon_N + \varepsilon_C)/2}$, where $\underline{X}_N$ = mole fraction of N terminal site bound (obtained by electrophoresis) and $\underline{X}_2 = 1 - \underline{X}_1$.

The iron removal reaction of an unmodified sample of 71% iron saturated transferrin was also monitored by urea-PAGE in combination with spectrophotometry. At various times during the reaction, 15 uL aliquots were withdrawn from the sample cuvette, mixed with an equal volume of 10% glycerol in electrophoresis tank buffer at pH 8.4, and immediately frozen in a dry ice/acetone bath. The high pH of the buffer effectively quenches the reaction. The buffer and PAGE procedure employed were as previously described (25). Approximately 10 ug of protein was applied to 1 cm slots and the electrophoresis was carried out at a constant 120 V for 24 hr at 4°C in a chromatography refrigerator. Coomassie Brilliant Blue R 250 stained gels were scanned

on a Hoefer GS 300 scanning densitometer interfaced to a MINC 11/23 laboratory computer for calculating the relative amounts of the four species of transferrin (i.e. apotransferrin, the C- and N-terminal monoferric transferrins, and diferric transferrin) present during the course of the reaction.

Under pseudo first-order conditions the iron removal reaction can be described by the following scheme:

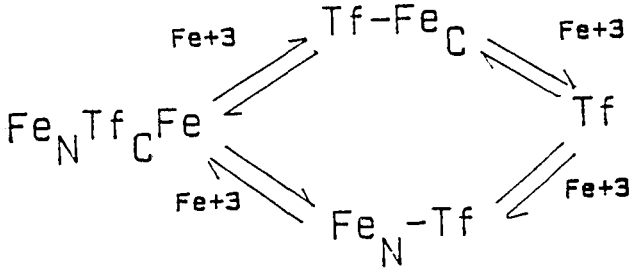

The coupled differential equations which describe the kinetics are given by equations 1.4 through 1.7.

$$\frac{d[D]}{dt} = -(k_{1,C} + k_{1,N})[D] \qquad (1.4)$$

$$\frac{d[N]}{dt} = k_{1,C}[D] - k_{2,N}[N] \qquad (1.5)$$

$$\frac{d[C]}{dt} = k_{1,N}[D] - k_{2,C}[C] \qquad (1.6)$$

$$\frac{d[A]}{dt} = k_{2,N}[N] + k_{2,C}[C] \qquad (1.7)$$

After rearrangement and integration expressions 1.8 through 1.11 are obtained for the time dependence of the concentrations of the four protein species, [D], [N], [C], and [A]. $[P]_o$ is the total protein concentration.

$$[D] = [D]_o \exp\{-(\underline{k}_{1,2} + \underline{k}_{1,N})t\} \tag{1.8}$$

$$[N] = \exp(-\underline{k}_{2,N}t) \cdot \left[\frac{\underline{k}_{1,C}[D]_o \exp\{(\underline{k}_{2,N} - \underline{k}_{1,C} - \underline{k}_{1,N})t\}}{\underline{k}_{2,N} - \underline{k}_{1,C} - \underline{k}_{1,N}} + [N]_o - \frac{\underline{k}_{1,C}[D]_o}{\underline{k}_{2,N} - \underline{k}_{1,C} - \underline{k}_{1,N}} \right] \tag{1.9}$$

$$[C] = \exp(-\underline{k}_{2,C}t) \cdot \left[\frac{\underline{k}_{1,N}[D]_o \exp\{(\underline{k}_{2,C} - \underline{k}_{1,C} - \underline{k}_{1,N})t\}}{\underline{k}_{2,C} - \underline{k}_{1,C} - \underline{k}_{1,N}} + [C]_o - \frac{\underline{k}_{1,N}[D]_o}{\underline{k}_{2,C} - \underline{k}_{1,C} - \underline{k}_{1,N}} \right] \tag{1.10}$$

$$[A] = [P]_o - [D] - [N] - [C] \tag{1.11}$$

The concentrations of the four species of transferrin obtained by scanning the gel was fitted to the equations 1.8 through 1.11 by a non-linear least square analysis to yield values for the four microscopic rate constants, $\underline{k}_{1,N}$, $\underline{k}_{1,C}$, $\underline{k}_{2,A}$, and $\underline{k}_{2,A}$.

Quantitation of Essential Residues

In order to quantitate the histidine residues involved in the iron release reaction for the individual sites, the Tsou Chen-Lu statistical method (21,26,39) was used to analyze the rate data for iron transferrin modified to different extents. In the present study the activity, $\underline{a}$, of a metal binding site was defined in terms of its macroscopic kinetic constants, i.e. $\underline{a} = (\underline{k}_p - \underline{k}_m)/\underline{k}_u$, where $\underline{k}_m$, $\underline{k}_u$, and $\underline{k}_p$ are the apparent first-order rate constants for iron removal from the fully modified, unmodified, and partially modified protein, respectively. The values of $\underline{k}$ for the two sites were determined by deconvolution of the spectrophotometric kinetic curves for the iron

removal reaction (equation 1.3). The statistical relationship between a and X, the mole fraction of unmodified residues within a pool of equally reactive histidines containing one or more essential residues, is given by $a^{1/i} = X$. A linear plot of $a^{1/i}$ vs. X is obtained for the proper choice of i (= 1, 2, etc.), the number of essential residues.

Kinetics of Iron Release as a Function of pH

Unmodified and modified (12.3 His/protein) 15 - 20 uM diferric transferrin solutions in 50 mM Hepes·Na/50 mM Mes·Na were adjusted to pH values in the range 5 - 7 with 1 N NaOH. The protein solution was placed in a dual beam recording Cary 219 spectrophotometer with the sample compartment thermostatted at 37°C and after equilibration was made 5 mM in citrate and 1.4 mM in desferrioximine B using stock 0.1 M citrate and 0.03 M desferrioximine B in the above buffer. The iron removal reaction was followed at 295 nm with a solution of apotransferrin and the other reagents serving as a blank. The rate constant k_2 was determined from the linear portion of the slow phase of the biphasic semilogarithmic plot.

EPR Spectroscopy

The X-band EPR spectra were measured on frozen solutions at 108°K as previously described (37). Spectra were double integrated over the scan range 500 - 2500 G.

RESULTS

Histidine modification of diferric transferrin greatly reduces the rate of iron removal from both binding sites by the mediating chelator pyrophosphate when desferrioximine B is employed as the terminal iron acceptor (vide infra). To elucidate this effect in detail, experiments were carried out to determine the number and relative reactivity of different histidine pools on the protein toward ethoxyformylation. These data were then used in conjunction with an analysis of the kinetics of the iron removal reaction of various modified transferrins. From the analysis, the pool containing the key histidines was identified. The number of such histidines in each metal binding domain was then inferred from Tsou Chen-Lu plots.

Ethoxyformylation of Diferric Transferrin

Diferric transferrin solutions (4.2 uM) can be partially modified (2.4 residues) or completely modified (14.8 residues) by varying the EFA concentration from 0.22 mM to 1.36 mM, respectively. In this context complete modification refers to all those histidines which are thought not to be ligands to the metal. According to the amino acid sequence there are a total of 18 histidine residues in human serum transferrin (14). Four of these are unreactive toward EFA in the presence of iron and presumably are coordinated to the metal (10). Our value of 14.8 reactive histidines on diferric transferrin compares with the previously reported value of 15.6 (10). These slightly high values probably reflect the analytical uncertainty in the spectrophotometeric method due to double ethoxyformylation of some residues at high degrees

of protein modification (40). No significant change in absorbance at 295 nm and 465 nm was observed upon modification, indicating that tyrosine modification and iron removal upon modification were minimal. Furthermore, the characteristic g' = 4.3 EPR signal of the diferric protein was relatively unchanged upon protein modification, suggesting that the metal coordination was unaltered (Fig. 1.1).

The time course of the modification reaction, along with the corresponding semilogarithmic plot, are shown in Figure 1.2. In accord with other studies (11), the reaction is distinctly biphasic, indicating the presence of two pools of histidines with significantly different reactivities toward EFA. The results of curve fitting according to equation 1.2 (Materials and Methods) indicate that there are 9 histidines in a fast reacting pool A ($\underline{X}_A$ = .61, $\underline{k}_A$ = 1.23 min^{-1}) and 5.8 in a slowly reacting pool B ($\underline{X}_A$ = .39 $\underline{k}_A$ = 0.28 min^{-1}). The numbers of histidines modified in each pool, N_a and N_b as a function of the total number of residues modified ($N_a + N_b$) were calculated from the relationship $1n[(9 - N_a)/9]/1n[5.8 - N_b)/5.8] = \underline{k}_a/\underline{k}_b$. The results are presented graphically in Figure 1.3. It is evident from the curves that a significant number of the histidines in pool B are modified only after ethoxyformylation of pool A histidines is nearly complete.

When the protein concentration is increased to 6.6 uM, only 11 histidines are modified per mole of protein at an EFA concentration of 1 mM. Increasing the EFA concentration to 5 mM causes no further modification. Kinetic analyses (Fig. 1.4) indicate that pools A and B, respectively, contain 9 histidines ($\underline{k}_a$ = 2.22 min^{-1}) and 2 histidines ($\underline{k}_b$ = 0.39 min^{-1}) under these conditions. Using the above kinetic data, numbers of histidines modified per pool as a

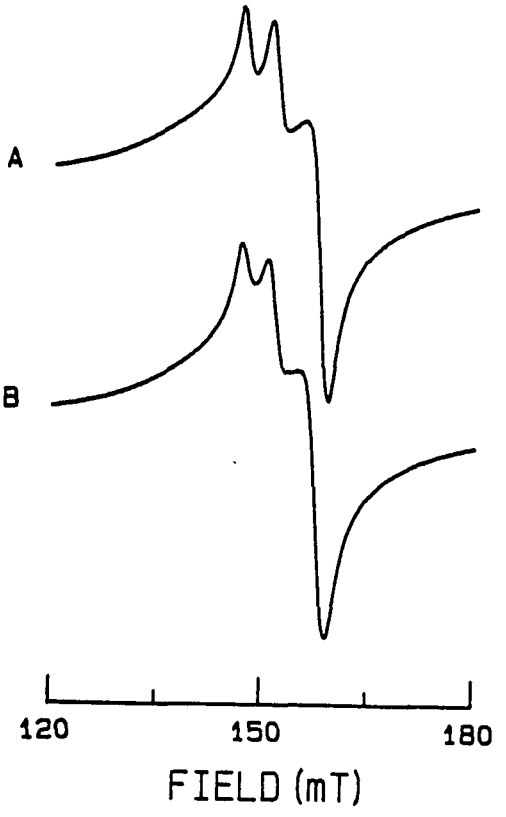

Fig. 1.1 g' = 4.3 EPR signals of diferric transferrin, 0.10 M Hepes·Na buffer, 0.01 M $NaHCO_3$, pH 7.4. A. unmodified, 0.22 mM in protein; B. extensively modified (10.6 His) with 10 mM EFA, 0.30 mM in protein.

Instrument parameters: scan range = 2000 G; field set = 1500G; time constant = 0.3 sec; scan time = 8 min; receiver gain = 1.25 X 10^2 (A), 1.6 X 10^2 (B); temperature = -165°C; microwave power = 80 mW; microwave frequency = 9.298 GHZ.

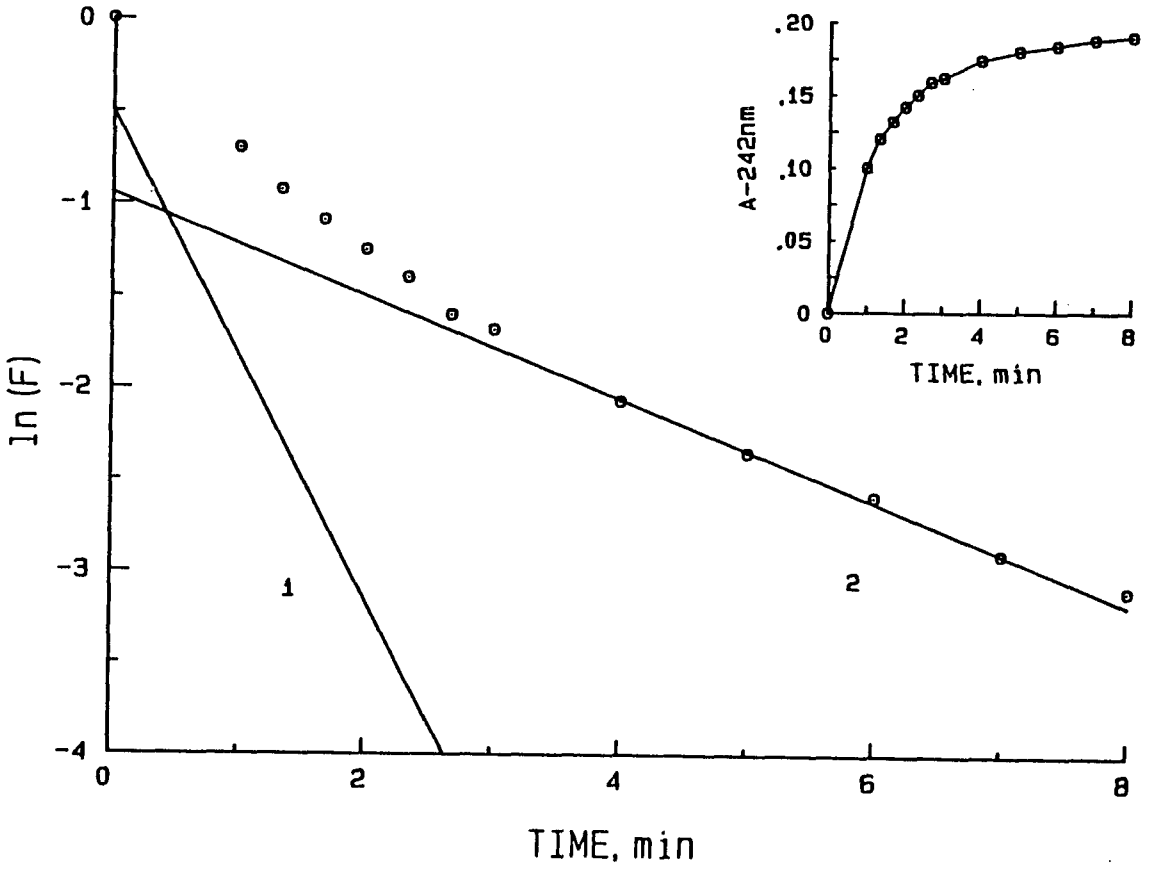

Fig. 1.2 Semilogarithmic plot of the fraction of histidines unmodified (F) vs. time for the ethoxyformylation reaction of diferric transferrin. Inset: absorbance at 242 nm vs. time. $F = (A_\infty - A_t)/A_\infty$. Conditions: 1.36 mM EFA, 4.2 uM transferrin, 0.1 M HEPES/Na, 0.02 M $NaHCO_3$, pH 7.3, 25°C. Straight lines were calculated using parameters obtained by curve fitting the data of the inset to equation 1.2, i.e. $X_A = 0.61$, $k_a = 1.23$, $X_B = 0.39$, and $k_b = 0.28\ min^{-1}$.

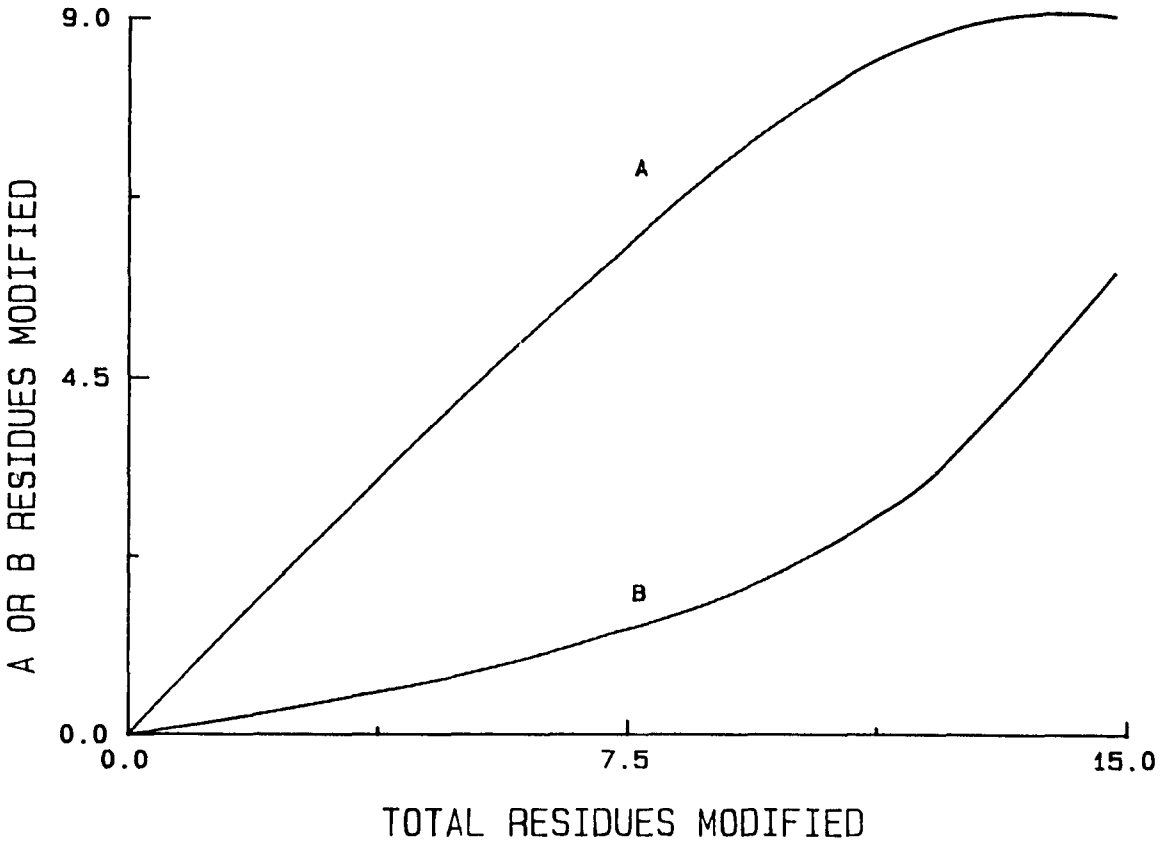

Fig. 1.3 Number of histidines in pools A and B as a function of the total number of histidines modified in diferric transferrin, based on kinetic parameters from reaction shown in Figure 1.2. See Materials and Methods and Results sections for details.

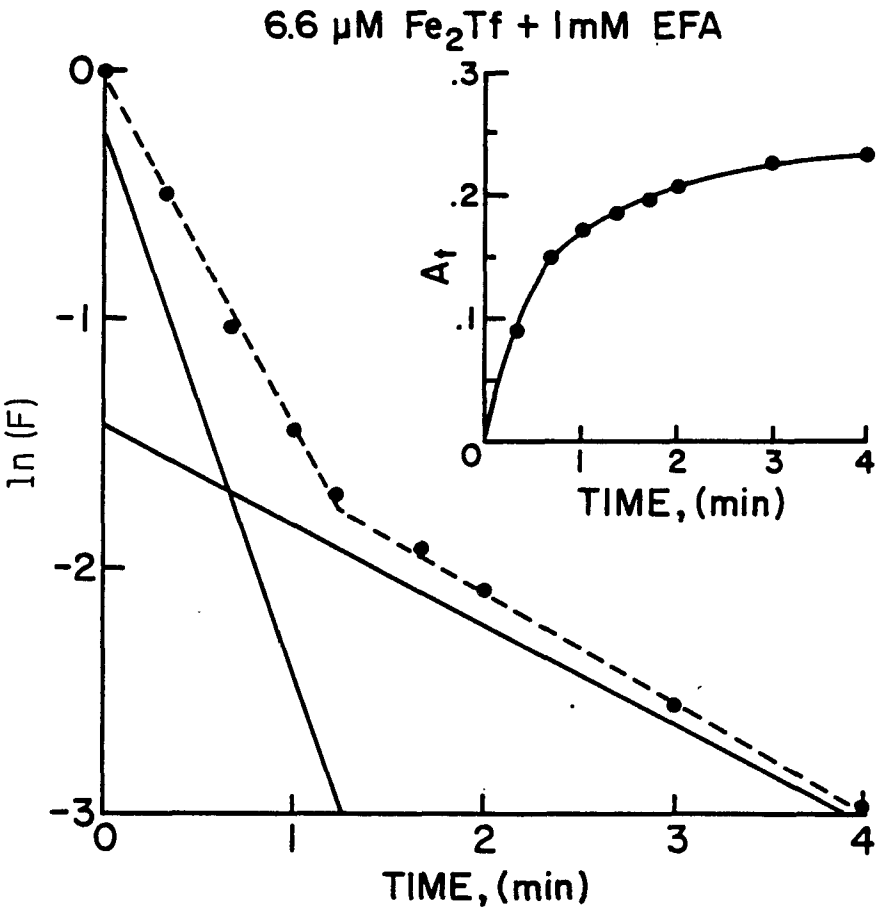

Fig. 1.4 Semilogarithmic plot of the fraction of histidines unmodified for the ethoxyformylation reaction of diferric transferrin as in Figure 1.2. Conditions: 1.0 mM EFA, 6.6 uM transferrin, 0.1 M HEPES·Na, 0.01 M $NaHCO_3$, pH 7.4, 25°C. Straight lines were calculated using parameters obtained by curve fitting the data of the inset to equation 1.2, i.e. $\underline{X}_A = 0.82$, $\underline{k}_a = 2.22\ min^{-1}$, $\underline{X}_B = 0.19$, and $\underline{k}_b = 0.39\ min^{-1}$.

function of total residues modified are shown in Figure 1.5. Thus, the reduction in the total number of histidines ethoxyformylated is the result of modification of fewer residues in the slowly reacting pool B. Protein samples modified at both protein concentrations were used in studies of the kinetics of iron removal from the protein.

The Iron Release Reaction

The kinetic curve for the removal of iron from unmodified 71% iron saturated transferrin at pH 6.9 and 37°C is shown in Figure 1.6. The experimental absorbance vs. time curve was deconvoluted into two components using equation 1.3 (Materials and Methods) to obtain the macroscopic first-order rate constants $\underline{k}_1$ = 0.19 min^{-1} and $\underline{k}_2$ = 0.032 min^{-1} (Fig. 1.3). These two rates correspond to iron removal from the N- and C-terminal binding sites, respectively (see below). Under the conditions of the experiment, the N-terminal site is the most labile (25).

The four microscopic kinetic constants for the reaction mixture studied spectrophotometrically in Figure 1.6 were obtained using urea-PAGE of reaction quenched samples (Materials and Methods). Figure 1.7 shows the variation in the mole percents of the four species of transferrin as a function of time for initially 71% iron saturated protein. The solid curves were calculated from equations 1.8 through 1.11 using the kinetic constants $\underline{k}_{1,N}$ = 0.18, $\underline{k}_{1,C}$ = 0.082, $\underline{k}_{2,N}$ = 0.27, and $\underline{k}_{2,C}$ = 0.028 min^{-1} which were derived from a non-linear regression fit of the data.

The semilogarithmic plot of the percent iron saturation of the protein versus time as determined from the gel data is shown in Figure

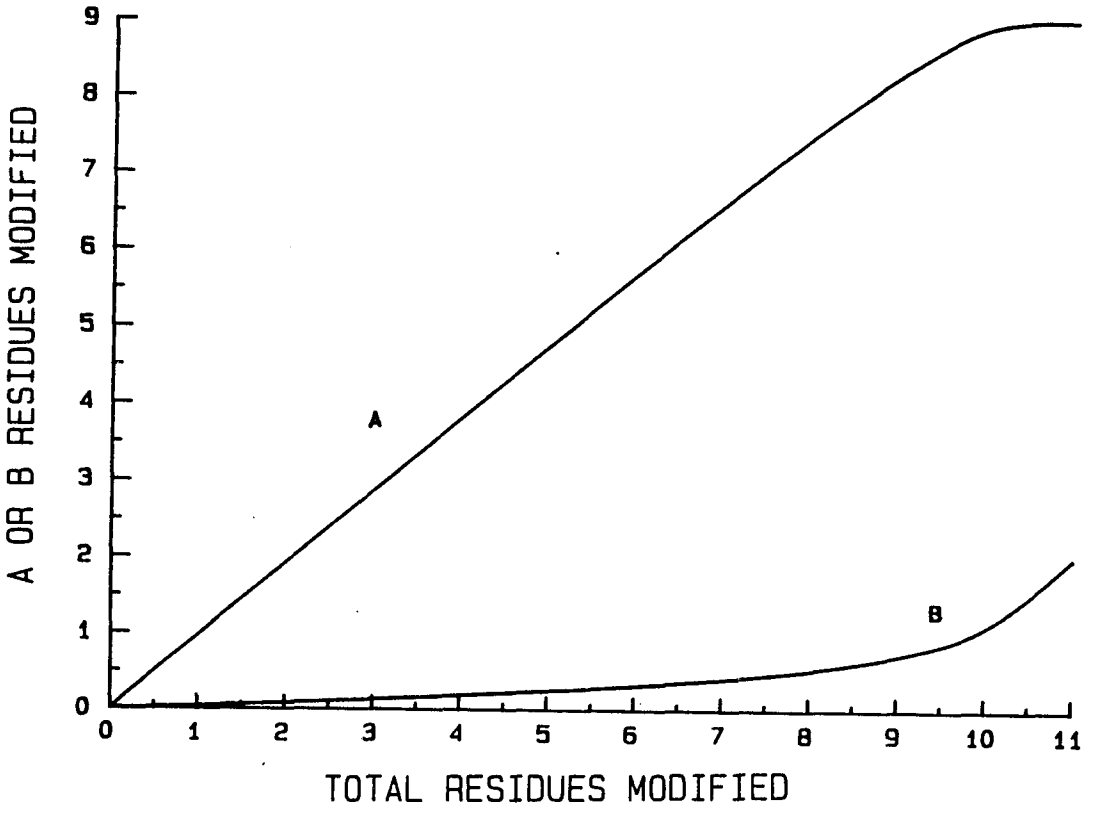

Fig. 1.5 Number of histidines in pools A and B as a function of the total number of histidines modified in diferric transferrin, based on kinetic parameters from reaction shown in Figure 1.4. See Materials and Methods and Results sections for details.

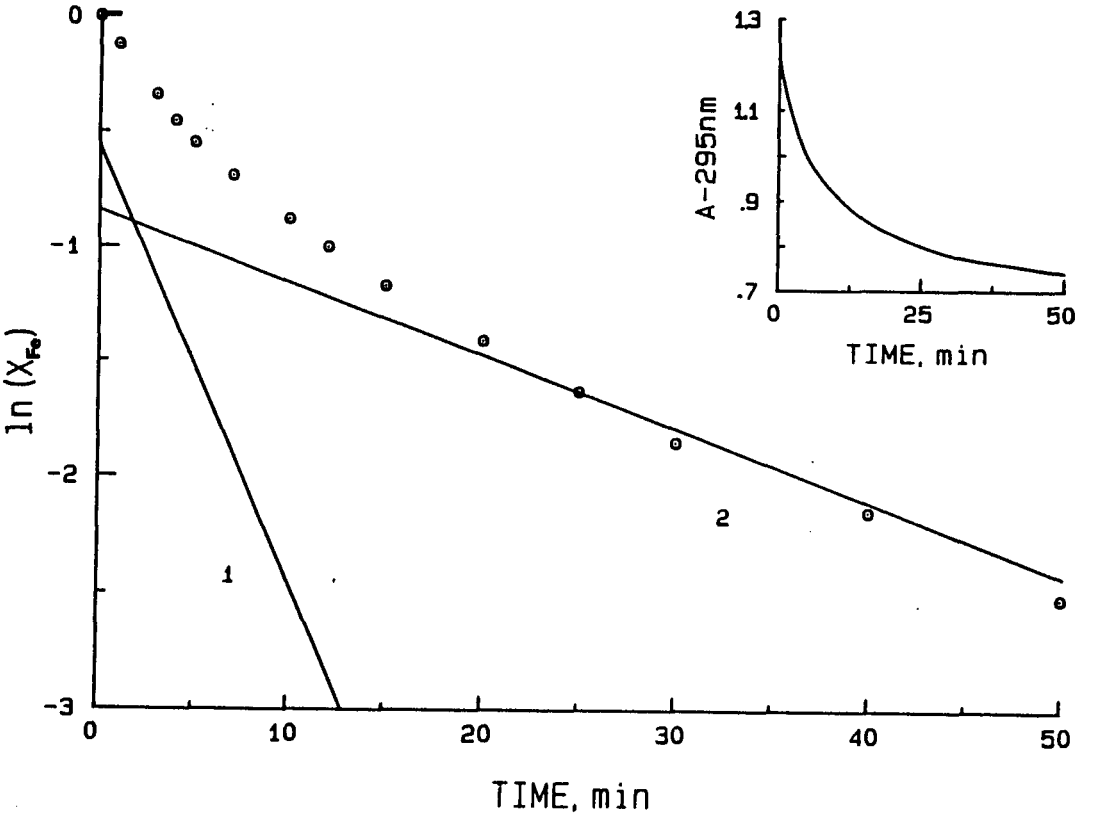

Fig. 1.6 Semilogarithmic plot of the fraction of iron bound (X_{Fe}) vs. time for the iron removal reaction of diferric transferrin. Inset: Absorbance vs. time. Conditions: 22.9 uM diferric transferrin (71% iron saturation), 3 mM pyrophosphate, 0.9 mM desferrioximine B, 0.1 M HEPES, 0.02 M $NaHCO_3$, pH 6.9, 37°C. The straight lines were calculated from parameters obtained by curve fitting the data in the inset to equation 1.3, i.e. $\underline{X}_1$ = .57, $\underline{k}_1$ = 0.19 min^{-1}, $\underline{X}_2$ = 0.43, and $\underline{k}_2$ = 0.032 min^{-1}. The two rates, 1 and 2, correspond to loss of iron from the N- and C-terminal binding sites, respectively. $\underline{X}_1$ and $\underline{X}_2$ are calculated, using values $\underline{X}_N$ = 0.6 and $\underline{X}_C$ = 0.4, and the appropriate molar absorptivities (see Materials and Methods).

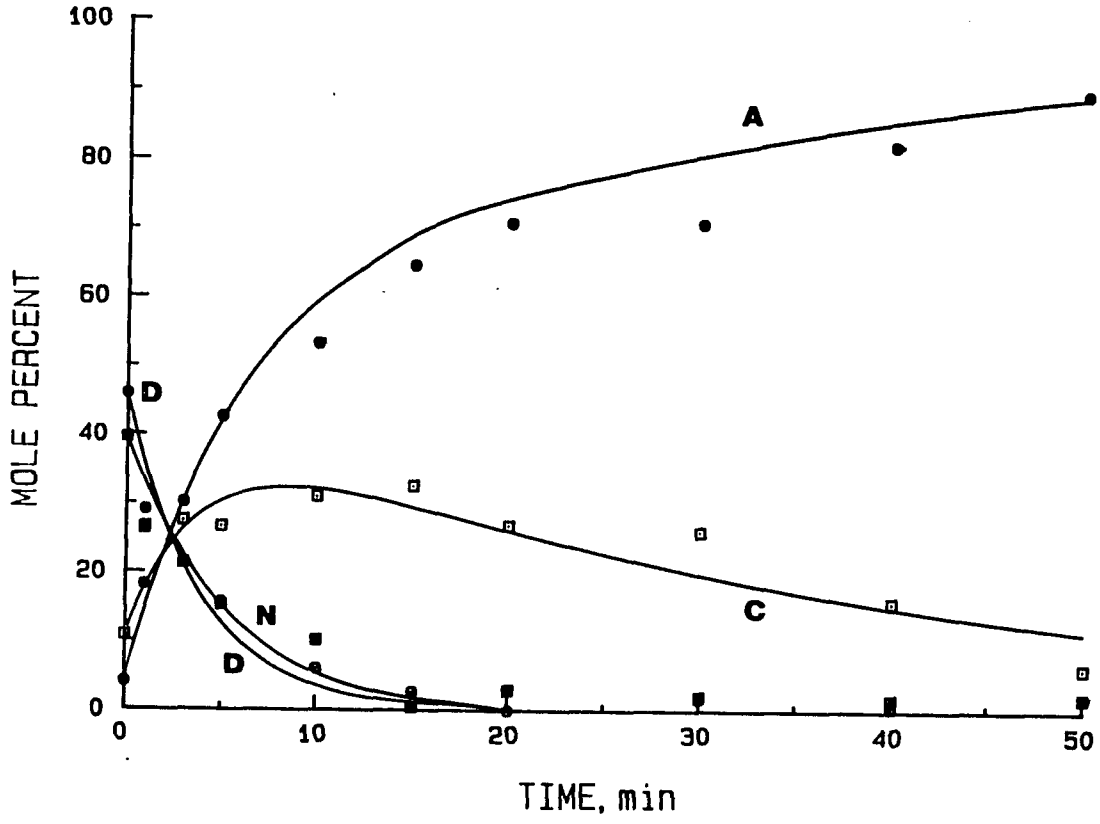

Fig. 1.7 Variation in the mole percent of the four species of transferrin as a function of time determined by urea-PAGE. Conditions same as in Figure 1.3. Solid curves were derived from curve fitting the data to equations 1.8 through 1.11 giving kinetic constants $\underline{k}_{1,N} = 0.18$, $\underline{k}_{1,C} = 0.082$, $\underline{k}_{2,N} = 0.27$, and $\underline{k}_{2,C} = 0.028$ min^{-1}. A = apotransferrin, N = N-terminal monoferric, C = C-terminal monoferric and D = diferric transferrin.

1.8. Although four microscopic kinetic constants describe the reaction, the curve is biphasic to a good approximation. The observed biphasic behavior is due to the insensitivity of the semilogarithmic plot to relatively small differences between the microscopic constants for each site ($\underline{k}_{1,N}$ vs. $\underline{k}_{2,N}$ and $\underline{k}_{1,C}$ vs. $\underline{k}_{2,C}$, see above).

In Figure 1.8 semilogarithmic plots for the percent saturation of the individual iron binding sites calculated from the gel data are shown. From the slopes, apparent rate constants of $\underline{k}_1$ = 0.18 and $\underline{k}_2$ = 0.034 min^{-1} for the two sites, respectively, are obtained. These values are in excellent agreement with the macroscopic constants $\underline{k}_1$ = 0.19 and $\underline{k}_2$ = 0.032 min^{-1} derived from the spectrophotometric data (Fig. 1.6), giving us confidence in the kinetic data and method of analysis.

Kinetics of Iron Removal from Modified Transferrins

Because quantitation of the effect of histidine modification on the rate of iron removal requires measurement of accurate rate constants, kinetic studies on a series of modified proteins were generally carried out using a single preparation of diferric transferrin which was stored lyophilyzed or in frozen solution at -13°C until needed for modification. The values of $\underline{k}_1$ and $\underline{k}_2$ for a total of 16 samples, either unmodified, partially modified, or fully modified, were obtained from deconvolution of the rate curves measured spectrophotometrically. Measurements were also made on modified and unmodified C-terminal monoferric transferrins to ensure that the smaller rate constant $\underline{k}_2$ of the modified diferric protein remained that of the C-terminal site.

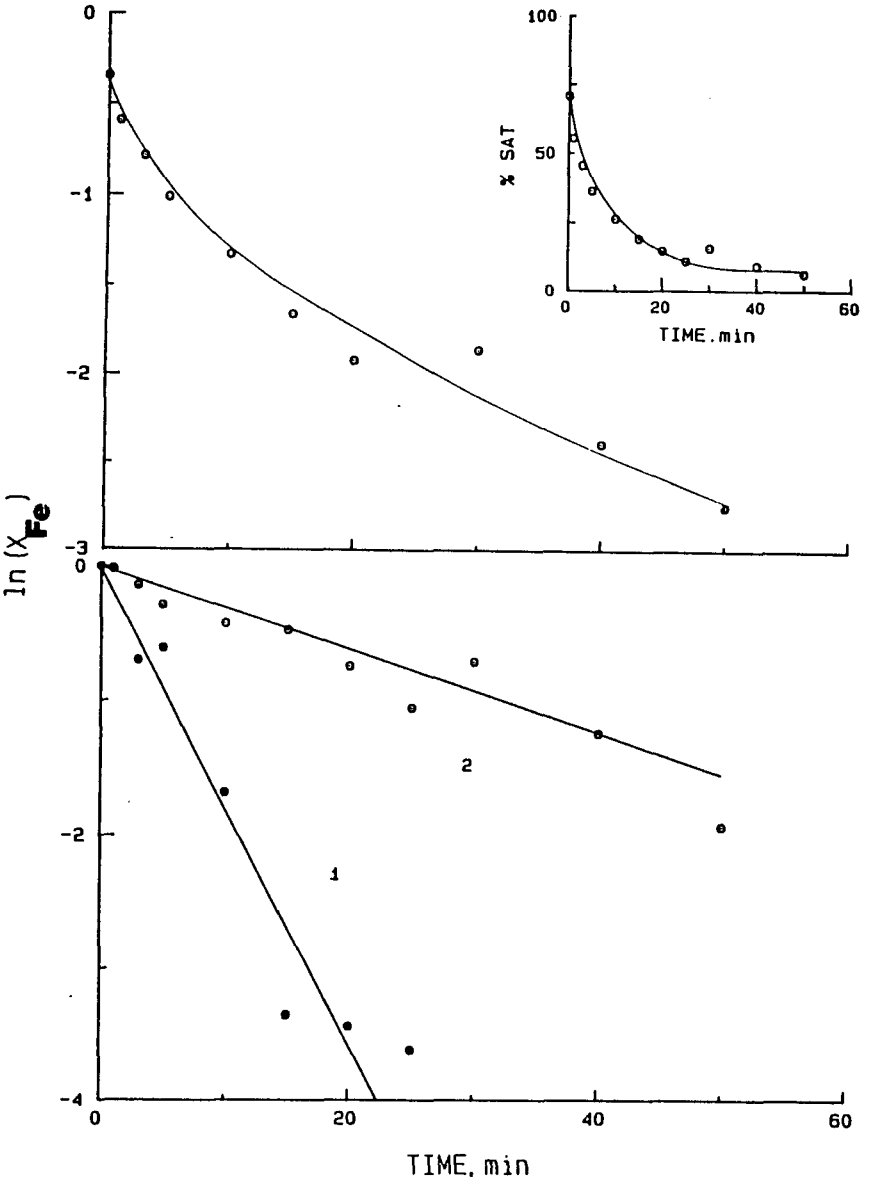

Fig. 1.8 Semilogarithmic plots of the fraction iron saturation of the protein as a function of time (upper curve) and fraction saturation of the N- and C-terminal binding sites as a function of time (lower curves) as calculated from urea-PAGE data in Figure 1.7. Inset: percent saturation of sample as a function of time calculated from the PAGE. The biphasic plot in (A) compares favorably with that in Figure 1.6 for the spectrophotometric data. Values of $\underline{k}_1$ = 0.18 and $\underline{k}_2$ = 0.034 min^{-1} obtained from the slopes of linear regression fits of the data in (B) are in good agreement with the values from Figure 1.6.

The dependence of k_1 and k_2 on histidine modification for samples ethoxyformylated at a protein concentration of 4.2 uM is shown in Figure 1.9. A linear decrease is observed for both rate constants, leveling off at about 12 histidines per mole of protein. Unmodified and partially modified (7 His) C-terminal monoferric samples showed rate constants for iron release of 0.069 and 0.031 min^{-1}, respectively. Similar linear plots (Fig. 1.10) are obtained for diferric samples modified at protein concentrations ranging from 6.0 to 10.0 uM. A comparison of the curves in Figures 1.3 and 1.9 shows that the reductions in k_1 and k_2 correlate with chemical modification of the fast reacting pool A histidines. Modification of pool B histidines has no apparent effect on the rate constants.

The data for the N-terminal site (from Fig. 1.9) on different modified transferrins is summarized in Figure 1.11 in the form of a Tsou Chen-Lu plot (Materials and Methods). Here X is the mole fraction of pool A histidines unmodified. The data in the form of the activity parameter, $a^{1/i}$, for both the N- and C-terminal binding sites vary linearly with X when i is chosen to be 1. The data plotted for i = 2 is decidedly curved. Higher values of i increase the curvature further. These results suggest that modification of a single histidine, presumably one in each iron binding domain, is responsible for the increased kinetic stability of the protein toward release of its iron.

Histidine modification likewise retards the rate of iron removal from both sites of ovotransferrin. Values of k_1 = 0.0086 min^{-1} and k_2 = 0.00024 min^{-1} were obtained for a partially modified (using 3 mM EFA) sample of ovotransferrin (4.3 His) compared to k_1 = 0.016

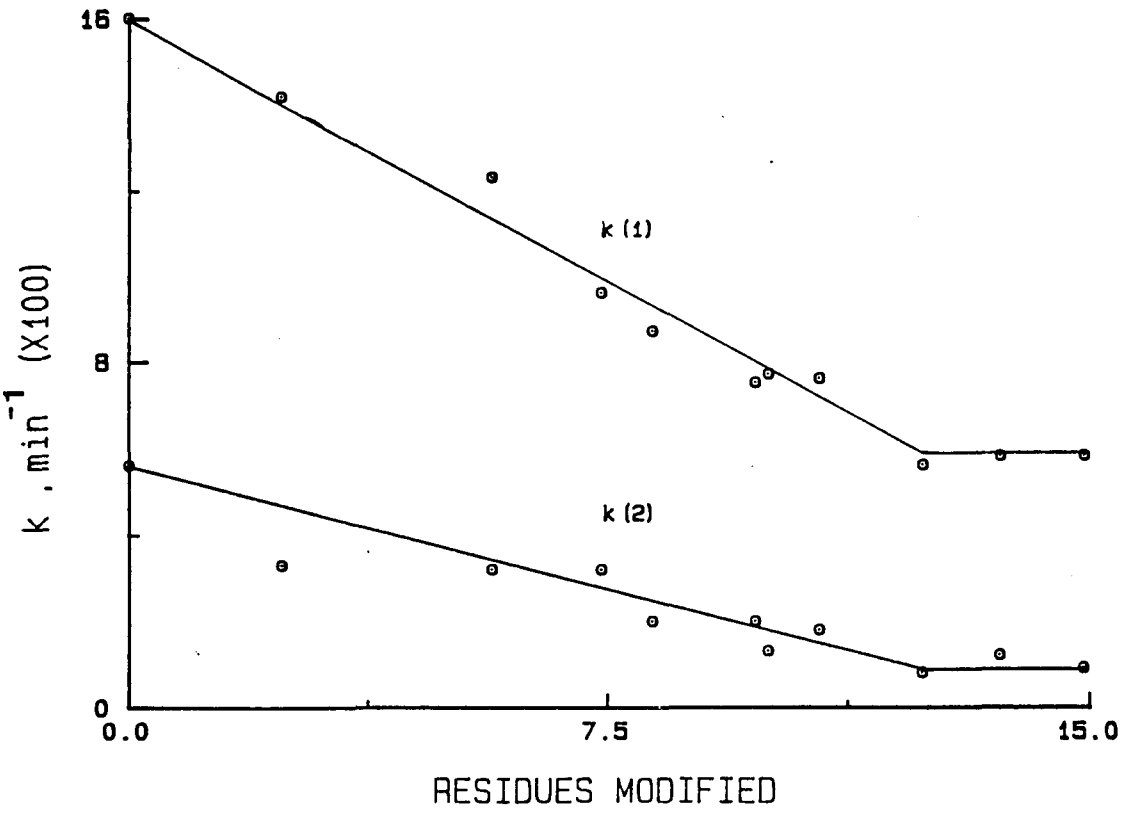

Fig. 1.9 Rate constants $\underline{k}_1$ and $\underline{k}_2$ for iron removal as a function of total number of histidines modified on diferric transferrin. A marked reduction in both rate constants is observed upon modification. Ethoxyformylation reaction carried out as described in Materials and Methods and in Figure 1.2. Conditions for the iron removal reaction as in Figure 1.6.

Fig. 1.10 Rate constants k_1 and k_2 for iron removal as a function of total number of histidine modification diferric transferrin Ethoxyformylation reaction carried out under conditions as in Figure 1.4. Iron release reaction carried out using 2 mM pyrophosphate and 0.3 - 0.4 mM desferrioximine B. Other conditions are the same as in Figure 1.6.

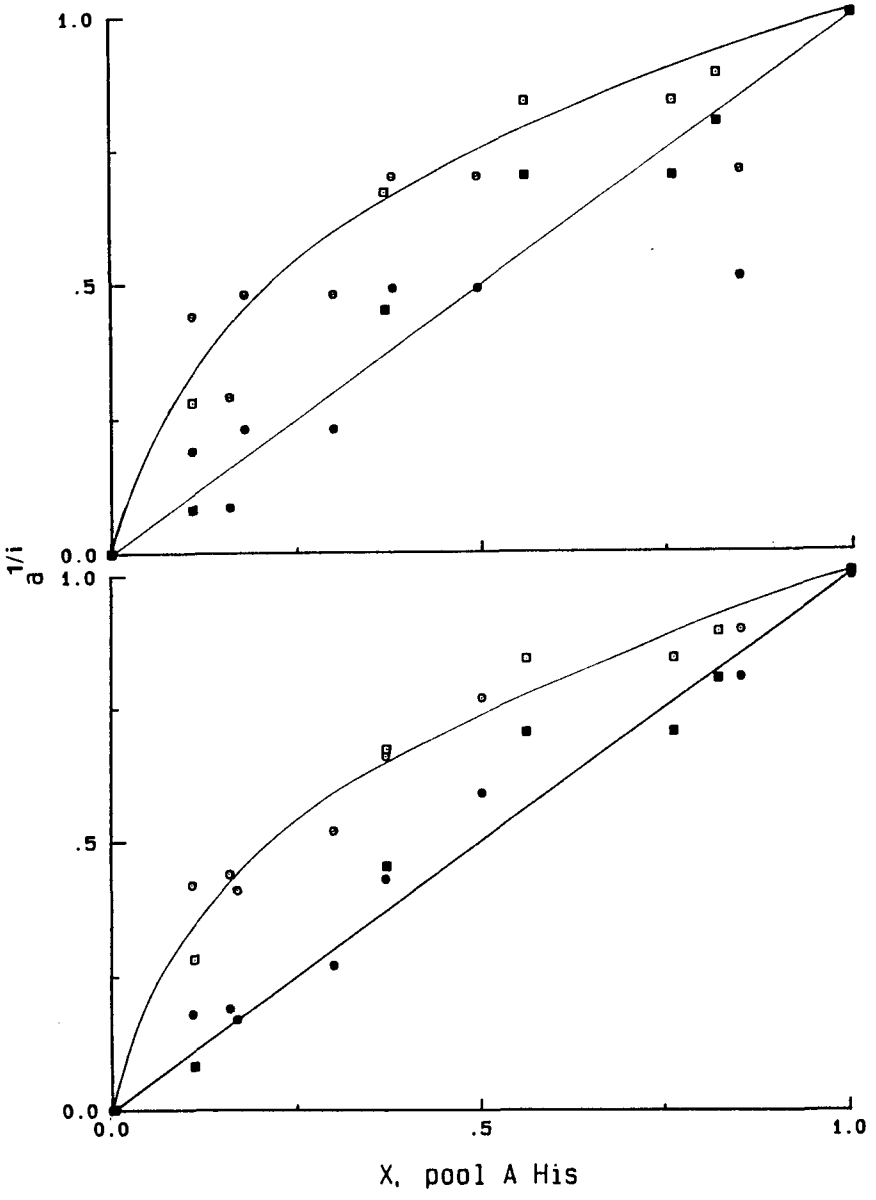

Fig. 1.11 Tsou Chen-Lu plots of the kinetic data for the N-terminal (upper) and C-terminal (lower) sites. (O) = data from Fig. 1.9 and (□) = data from Fig. 1.10. Solid and open symbols designate i = 1 and i = 2 plots, respectively. See Materials and Methods for definition of activity a (see Results).

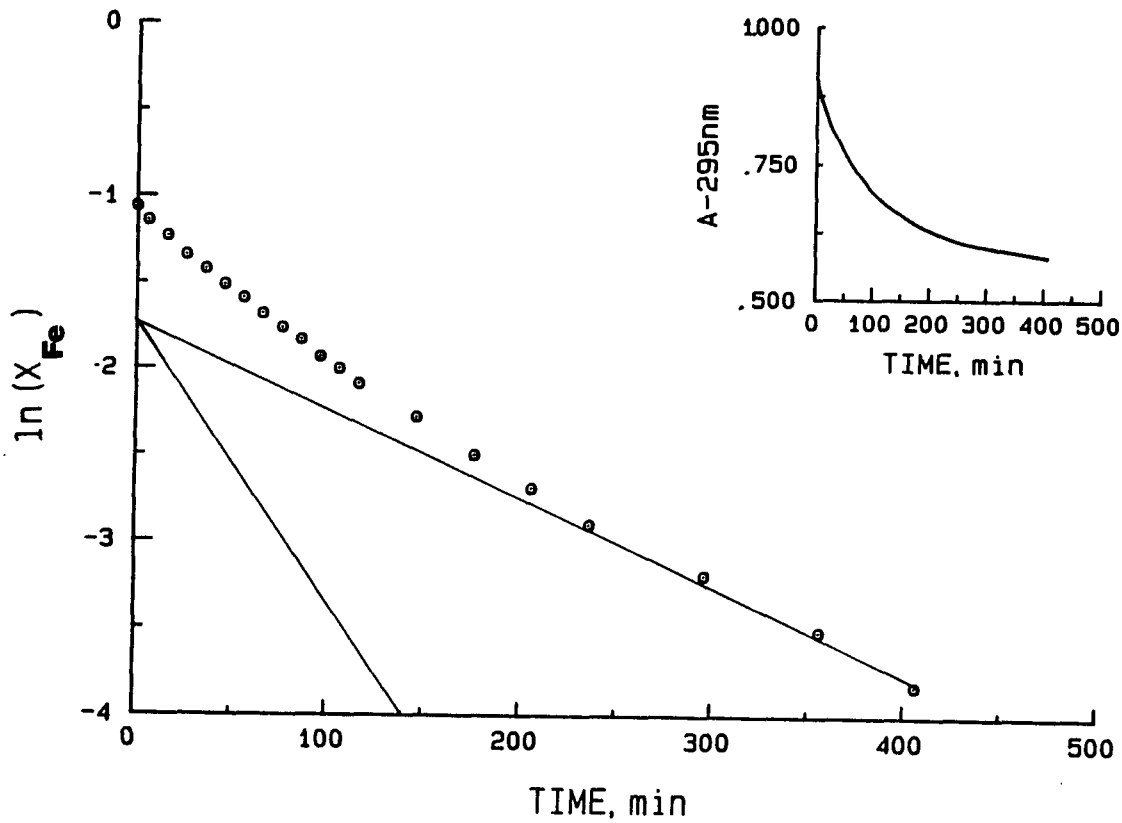

Fig. 1.12 Semilogarithmic plot of the fraction of iron bound (X_{Fe}) for the iron removal reaction of 17 mM diferric ovotransferrin. Conditions same as in Figure 1.6.

min^{-1} and $\underline{k}_2$ = 0.005 min^{-1} for the native protein (Fig. 1.12). Ovotransferrin is known to react less extensively with EFA than human serum transferrin (10,11). A similar study with modified (7 His), using 3 mM EFA, and native lactoferrins carried out at pH 5.35 gave initial rates of iron release of 0.0016 and 0.0012 min^{-1}, respectively. Thus, modification of lactoferrin has actually accelerated on the kinetics of iron removal by a small amount.

Dependence of the Rate of Iron Removal on pH

The rate of iron removal from transferrin by chelators is known to be greatly accelerated when the pH is reduced below 7.0 (41). The pH dependence of $\underline{k}_2$ for unmodified and extensively (12.3 His) protein samples using citrate as a mediating chelating agent is shown in Figure 1.13. It is evident from the two curves that modification greatly increases the kinetic stability of transferrin iron below pH 5.5. The rate of iron removal at pH 5 has also been studied using the mediating chelators pyrophosphate, orthophosphate, DPG, ATP, and GTP (47). In all cases modification renders the transferrin iron complex more kinetically stable.

A plot of $\log(\underline{k}_2)$ vs. pH (Fig. 1.13 inset) for the unmodified protein is linear with a slope of -0.94, a result consistent with the findings of others (41). The fact that the H^+ dependence is largely quenched in the modified protein suggests that an imidazole group of histidine may be the proton acceptor in this reaction.

Electron Paramagnetic Resonance Spectrum

The influence of salts on the EPR spectrum of the modified protein was investigated. It is well known that the addition of chloride

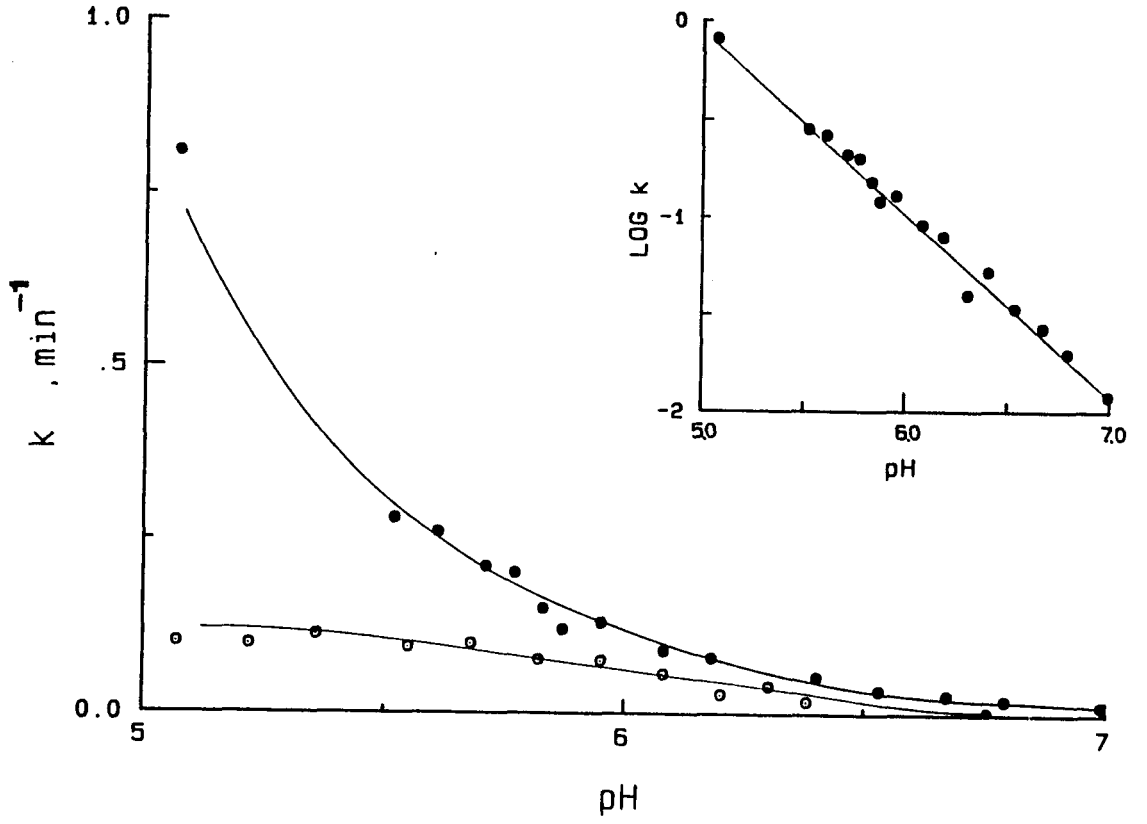

Fig. 1.13 pH dependence of $\underline{k}_2$ for native (•) and modified (∘) diferric transferrins. Inset: Log$\underline{k}_2$ vs. pH for the native protein. A slope of -0.94 is obtained. Conditions: 15 - 20 uM protein, 5 mM sodium citrate, 1.4 mM desferrioximine B, 50 mM HEPES·Na, 50 mM MES·Na, pH adjusted between 5 and 7, 37°C. Rates were generally measured at 37°C; however, the pH 5 data point for the native protein was measured at 25°C (to slow rate for convenient monitoring of the kinetics) and subsequently corrected for the temperature dependence in the rate.

(0.5 M) to solutions of native diferric transferrin produces a shoulder on the low field side of the g' = 4.3 doublet (32). Addition of perchlorate at the same concentration causes partial loss of resolution in the doublet (30,32a). These effects have been attributed to anion binding to the protein (32). Although we observed little change in the EPR spectrum upon histidine modification (Fig. 1.1), the effect of chloride on the EPR signal was no longer present in the modified protein. Figure 1.14 shows the g' = 4.3 EPR spectra of (A) native and (B) ethoxyformylated (10.6 His/mole) diferric transferrin in the presence of 0.5 M NaCl. However, the perchlorate effect was still manifested (Fig. 1.15).

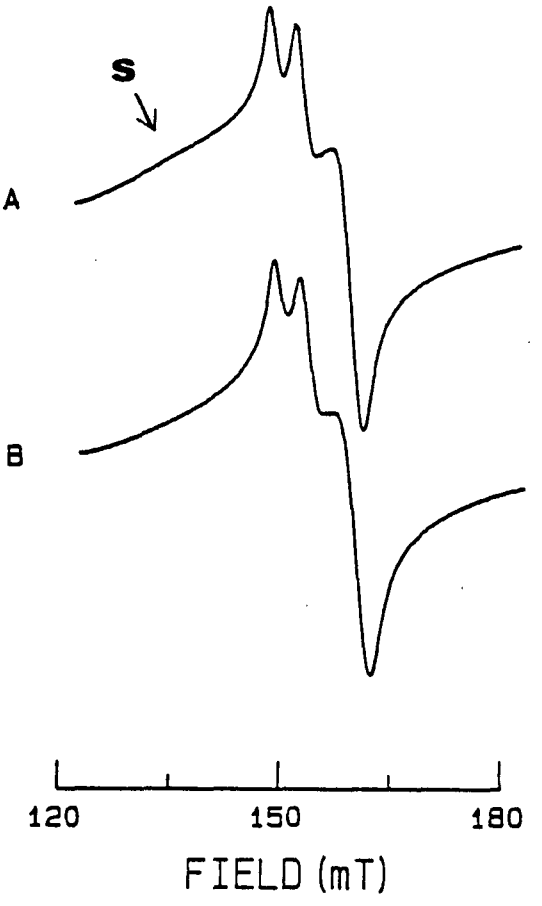

Fig. 1.14 g' = 4.3 EPR signals of diferric transferrin, 0.5 M NaCl, 0.1 M HEPES·Na, 0.01 M $NaHCO_3$, pH 7.4. (A) RG 160 unmodified, (B) RG 160 extensively modified (10.6 His). All other conditions and instrumental parameters same as in Figure 1.1.

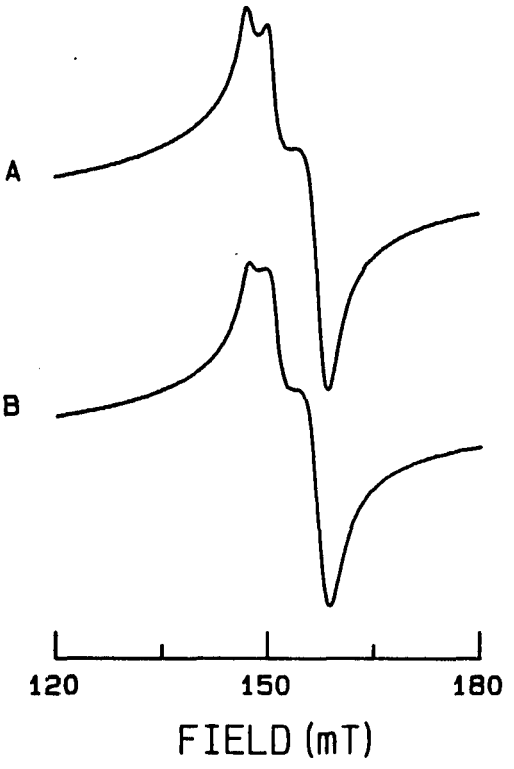

Fig. 1.15 $g' = 4.3$ EPR signals of diferric transferrin, 0.5 M $NaClO_4$, 0.1 M HEPES·Na, 0.01 M $NaHCO_3$, pH 7.4. (A) RG 160 unmodified, (B) RG 160 extensively modified. All other conditions and instrumental parameters same as in Figure 1.1.

DISCUSSION

The first-order dependence of the rate of iron release from transferrin on proton concentration suggests that proton transfer occurs prior to or during the rate limiting step for the reaction. This observation and interpretation have been previously published (41). Further evidence for the involvement of the protonation step in transferrin-iron removal comes from *in vivo* studies. In the immature erythroid cell, there is strong evidence that transferrin is internalized into a low pH (about 5) vacuole, where the iron is released to an acceptor (42,43), possibly citrate or adenosine triphosphate.

The specific role of the hydrogen ion in the labilization of transferrin iron is unclear; however, several possibilities present themselves: (1) protonation of a protein ligand, carbonate, or hydroxide on the metal, (2) a local conformational change induced by protonation of one or more amino acids surrounding the metal, but not coordinated to it, and (3) direct binding of the mediating chelating agent at a positively charged anion-binding site, produced by protonation of an amino acid functional group near to the metal. It is likely that more than one of these mechanisms are operating over the wide pH range employed here. Of these three possibilities, (1) would not be affected by ethoxyformylation. Clearly, the iron ligands are protected from EFA by the intact metal (10). Possibilities (2) and (3) likely explain the retarded rates of iron release in the modified

transferrins. However, neither of these possibilities can be ruled out.

The acid stability to iron release observed in the fully modified transferrin is evidence that a protonated histidine is involved in the citrate mediated reaction. Over a wide, physiological pH range, transferrin-iron is stabilized by modification. The stability is greatest below pH 6.0, where histidine is normally titrated in proteins, i.e. pK_a ~6.9 (44). This observation is of relevance to the in vivo studies already discussed. Likewise, at pH 7 the modification offers less kinetic stabilization.

The pH profile of the rate constant for the modified protein has a titration-like appearance with an apparent pK_a ~5.7. Possibly this trend is a reflection of the mediating anion, citrate, which has a second acid dissociation of $10^{-5.82}$ (45). This possibility is not easily proven, but suggests that the monoanionic form of citric acid is an ineffective mediator but that the di- and tri-anionic species are both effective. This trend is not observed in unmodified transferrin and suggests that the iron release reaction pathway is significantly altered due to the chemical modification of histidine.

The observed decline in the rate of iron release upon ethoxyformylation may be due to several reasons: (1) the introduction of an ethoxyformyl group could obstruct entry of the mediating anion to the metal site or sterically hinder protein unfolding that occurs as transferrin gives up its iron; (2) the ethoxyformyl group may be effectively neutralizing a positive charge on the protein that facilitates iron release either by influencing the native conformation of transferrin or providing a binding site for the mediator anion. The

fact that histidine modification removes the effect of Cl^- argues for a role of histidine in anion binding and/or conformational stability of the protein. We favor the second possibility, in light of the pH studies which suggest that charge, not stereochemical considerations are probably the governing influence in the labilization of transferrin iron.

The data suggest that one non-liganded histidine per domain is involved in the iron release reaction. A string model of the proposed metal and anion binding locus of human serum transferrin and ovotransferrin show the presence of three conserved histidines per domain (His·119, His·207, and His·249 in the N-domain). Two of these residues probably coordinate directly to the metal (10,33). The remaining histidine may well be the residue targeted in this study. His·207 is not conserved in lactoferrin (46), a transferrin with unusual acid stability (41) and which exhibits an enhanced rate of iron removal by histidine modification (see Results). Interestingly, the 207 position of lactoferrin is occupied by a negatively charged, glutamic acid residue. A single, titratable histidine, proximal to the metal, may provide the key to understanding the unusual kinetic and thermodynamic properties of human serum transferrin iron. An amino acid with such an important physiological role might well be conserved throughout evolution.

The results of this study are by no means conclusive. However, our results are in agreement with other reports that the hydrogen ion is intimately associated with transferrin iron uptake and release. Our studies further indicate that the protein backbone, including one non-liganded histidine participates in the iron removal reaction, the

effect being most pronounced at pH values where histidines are expected to be protonated. Further work is needed to identify the histidine, characterize its environment, and determine its distance from the metal. X-ray structural analysis will ultimately resolve these issues and shed new light on the iron-exchange processes of transferrin.

CHAPTER II

KINETIC AND SPECTRAL STUDY OF LYSINE-MODIFIED HUMAN SERUM TRANSFERRIN

INTRODUCTION

String models of various transferrins show that there are several cationic amino groups in the regions of the proposed metal binding sites (33). Groups conserved between the two domains of human serum transferrin include Lys 115, Lys 116, Lys 206, Lys 217, Lys 233, Arg 124, Arg 232, and Arg 254 (in the N-domain). The effects of simple salts such as sodium chloride and sodium perchlorate on the EPR spectra of the iron centers (26,30,32) and on the kinetics of iron removal (24,27,28) may be partially due to the proximity of these potential anion binding sites to the metal. It is noteworthy that several non-conserved lysines are also present, i.e. Lys 144, Lys 193, Lys 196, and Lys 239 in the N-domain with C-domain counterparts Phe 476, Arg 522, and Ala 574, and in the C-domain Lys 470, Lys 498, Lys 490, Lys 511, Lys 527, Lys 557, and Lys 590 with N-domain counterparts Asp 138, Thr 165, Asp 166, Ala 199, Gln 122, and Ser 255. These non-conserved residues likely play a role in the differential response to salts between the two domains, observed both kinetically and spectroscopically.

The oldest method for chemically modifying lysine residues in proteins is the acetylation reaction with acetic acid anhydride. The product of the reaction of the amino group and acetic acid anhydrides is the corresponding amide, which is unprotonated at neutral pH (48). Modification of arginine groups is accomplished with phenylglyoxal (12,48), also yielding a neutral product.

In the present study, the spectral and kinetic "salt" effects are studied using chemical modification. Our data suggest that lysine and possibly arginine residues make up or are located near the perchlorate binding sites of human serum transferrin.

MATERIALS AND METHODS

Iron free human serum transferrin of 98% stated purity was purchased from Calbiochem Co. To ensure that the commerical preparation was free of anionic contaminants, the protein was dissolved in a previously chelexed solution of 0.5 M $NaClO_4$ and 0.02 M $NaHCO_3$, pH 8.7 and then dialyzed against 0.02 M $NaHCO_3$, pH 9.0. The protein was assayed and made diferric as described earlier in Chapter I.

C-terminal monoferric transferrin was prepared using $Fe(NTA)_2$, as outlined previously in Chapter 1. N-terminal monoferric transferrin was prepared as described earlier (50), with minor changes. A 0.1 mM diferric transferrin solution (93% iron saturated) in 0.1 M HEPES·Na, 0.02 M $NaHCO_3$, and 0.5 M in $NaClO_4$, at pH 7.8 was made 1 mM in pyrophosphate (Sigma) and desferrioximine B (Ciba). The solution was allowed to stand at room temperature for approximately four hours. Excess reagents and low molecular weight reaction products were separated from the protein solution by ultrafiltration with a Model 10 Amicon cell fitted with a PM 10 membrane (molecular weight exclusion limit nominally 10,000) using several changes of fresh iron free bicarbonate buffer. The N-terminal monoferric preparation was assayed using urea-PAGE and stored frozen in solution at -13°C. The electrophoresis gels showed approximately equal amounts of apo and N-terminal species. No C-terminal or diferric protein was detected visually.

Modification of lysine residues was achieved by the method of Conrat and Fraenkel, with minor variations (53). To a rapidly stirring solution of 2 ml 0.1 - 0.2 mM protein/0.1 M $NaHCO_3$ (chelexed)

solution, pH 9.0 was added 2 - 20 microliter quantities of reagent grade acetic acid anhydride (Baker Analyzed) in several additions. After each addition, 1 M NaOH (Baker) was added to maintain constant pH. Modified samples were ultrafiltered against 3 volume changes (90% volume reduction per change) of fresh iron free 0.1 M HEPES buffer, pH 7 to remove low molecular weight reaction products. Extent of modification was assayed by means of the trinitrobenzene sulfonic acid method of Habeeb (49) using an unmodified protein sample as a control.

The arginine modification reaction was carried out by incubating 40 uM diferric transferrin with 20 mM phenylglyoxal in 0.1 M $NaHCO_3$, pH 8.7 for 6 hr. Reagents were removed by ultrafiltration. The extent of modification was determined by amino acid analysis, performed by University Instrumentation Center.

All EPR spectra of modified and native protein samples were measured at X-band frequency at 77°K, unless otherwise noted, in calibrated quartz EPR tubes (i.d. ≅ 3 mm, o.d. ≅ 4 mm), digitized, and stored on floppy disk. Double integrations were done over the entire 200 mT scan range centered at 150 mT to ensure that all of the Fe(III) was EPR observable upon addition of salts (32a) or modification of the protein.

Iron release studies were performed as described in Chapter I. Pseudo-first order rate constants were determined for the C-terminal monoferrics by taking the slope of the semilogarithmic absorbance-time data. In the case of the diferric protein, rate constants of the individual sites were extracted by deconvolution of the spectrophotometric data as detailed in Chapter I. Urea-PAGE was employed as described in detail in Chapter I.

RESULTS

The effect of 0.5 M NaCl, 0.5 M $NaClO_4$, and a mixture of the two on the EPR spectrum of 80% saturated transferrin is shown in Figure 2.1. Three effects are evident. First, the addition of either salt causes a reduction of 30 - 40% in the EPR amplitude and a 15 - 20% reduction in the double integral of the spectrum, evaluated between the limits of 60 mT and 230 mT. Secondly, chloride produces a shoulder on the low field side of the spectrum designated S in Figure 2.1. Thirdly, perchlorate causes the doublet feature (labelled D at the top of the signal) to partially coalesce from 4.1 mT to 2.7 mT, but no prominent shoulder is produced. Baldwin et al. (24) have likewise failed to observe a shoulder in the EPR of diferric transferrin in the presence of perchlorate and have suggested that the shoulder reported by Price and Gibson many years ago (30) may have been due to non-specifically bound iron in their sample preparations.

Figures 2.2 and 2.3 show the $g' = 4.3$ EPR signals of C- and N-terminal monoferrics and the effect of added salts, sodium chloride, and sodium perchlorate. The differential effect of salts on the two sites is apparent, as has been reported previously (24). The salient features of the perchlorate effect upon the C-terminal monoferric signal (Fig. 2.2B) are a 44% reduction in peak to peak amplitude, a 35% decrease in double integral and coalescence of the transferrin doublet feature into a broad singlet. Sodium chloride produces no major change in signal shape, but a 38% reduction in peak to peak amplitude and an 8% reduction in double integral (Fig. 2.2C).

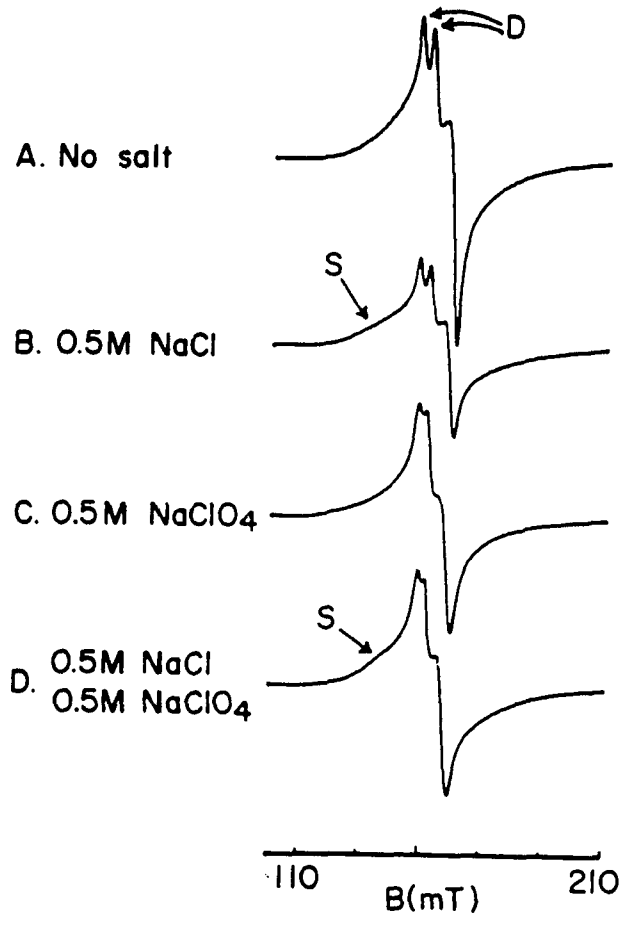

Fig. 2.1 Frozen solution EPR spectra of 80% iron saturated transferrin, in 0.1 M HEPES·Na buffer, 0.02 M $NaHCO_3$, pH 7.4, in presence of various salts. Instrument parameters: scan range = 2000 G, field set = 1500 G, time constant = 1.0 sec, scan time = 16 min, modulation amplitude = 10 G, modulation frequency = 100 kHz, receiver gain = 320, temperature = 108°K, microwave power = 80 mW, and microwave frequency = 9.30 GHz.

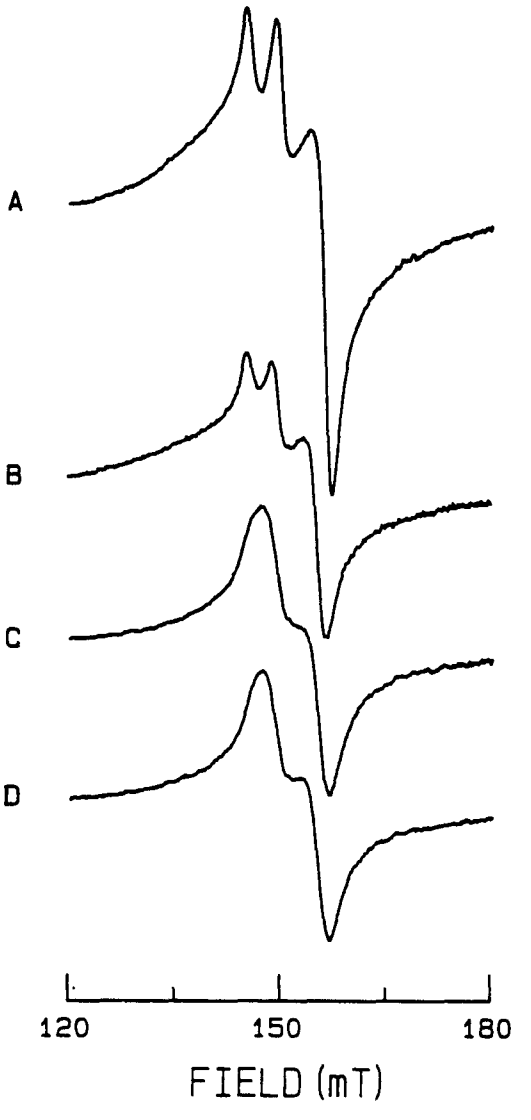

Fig. 2.2 Frozen solution EPR spectra of C-terminal monoferric transferrin (0.21 mM in iron) in 0.1 M HEPES·Na, 0.02 M $NaHCO_3$ buffer, pH 7.5, in A. no salt; B. 0.57 M NaCl, C. 0.54 M $NaClO_4$; D. 0.48 M NaCl, 0.48 M $NaClO_4$. Instrument parameters: scan range = 2000 G, field set = 1500 G, time constant = 1.0 sec, scan time = 8 min, modulation amplitude = 10 G, modulation frequency = 100 kHz, receiver gain = 1000, temperature = 77°K, microwave power = 20 mW, and microwave frequency = 9.145 GHz.

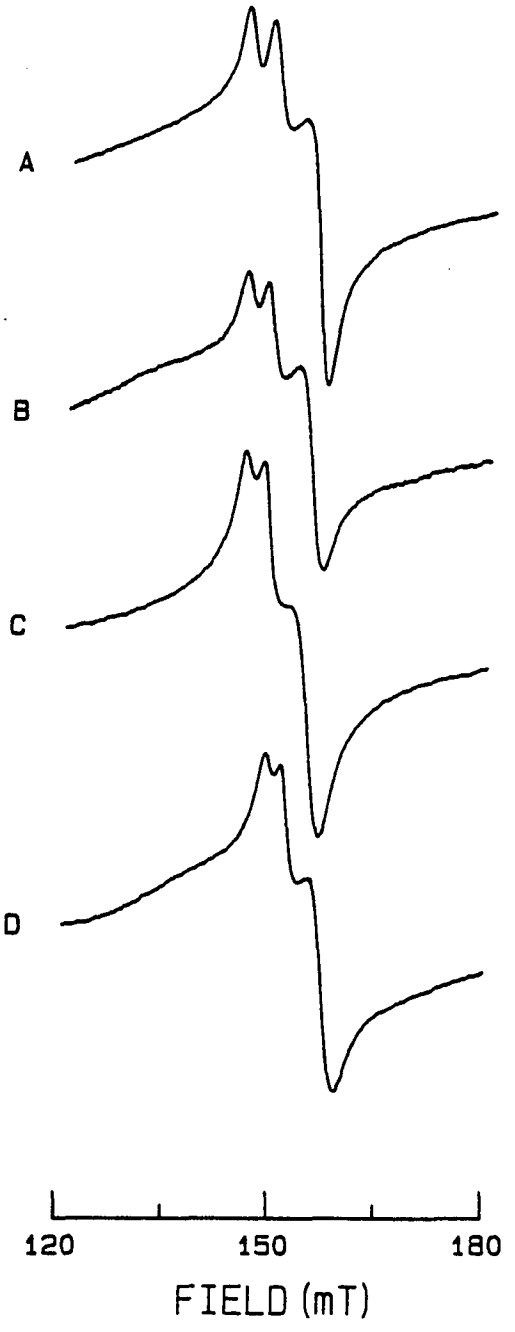

Figure 2.3 Frozen solution EPR spectra of N-terminal monc :rric transferrin (0.24 mM in iron) in 0.1 M HEPES·: , 0.02 M $NaHCO_3$ buffer, pH 7.5, in A. no salt; B. 0.50 NaCl; C. 0.50 M $NaClO_4$; and D. 0.45 M NaCl, 0.45 M NaCl . Instrument parameters same as in Fig. 2.2 exce receiver gain = 1250 and microwave frequency = 9.112 G .

The N-terminal signal is also affected by perchlorate treatment (Fig. 2.3C), but less extensively. There is a small amount of doublet coalescence; but, no reduction in peak to peak amplitude and only an 8.8% reduction in the double integral. Sodium chloride (Fig. 2.3B) caused a shoulder to develop at the low field side of the N-terminal signal and a 19% and 22% reduction in amplitude and double integral, respectively. Also, a small doublet coalescence similar to that caused by perchlorate addition was observed. The spectral "salt effects", i.e. doublet coalescence, the appearance of a shoulder, and the reduction in amplitude, characteristic of the diferric protein (26,30,32), can be individually and quantitatively accounted for as the sum of the individual monoferric signals as shown in Figure 2.4. These experiments also confirm that the NaCl and $NaClO_4$ induced spectral changes observed in diferric transferrin essentially arise from separate domains of the protein.

The influences of chloride and perchlorate individually on the EPR spectrum were studied as a function of pH. The spectral changes shown in Figure 2.1 for pH 7.4 were also largely present at pH 11.2, suggesting that cationic groups with high pK_a values are involved in the binding of these anions. The reduction in the doublet splitting due to perchlorate as a function of pH is given in Table 1.

The EPR spectrum of the lysine modified protein is remarkably similar to that of the native protein in the presence of perchlorate (c.f. Fig. 2.1C and Fig. 2.5 Lys). The spectrum of the arginine modified protein is less so, but the protein is only 50% modified. These data suggest that the coalescence of the doublet feature may simply arise from neutralization of positively charged groups, i.e.

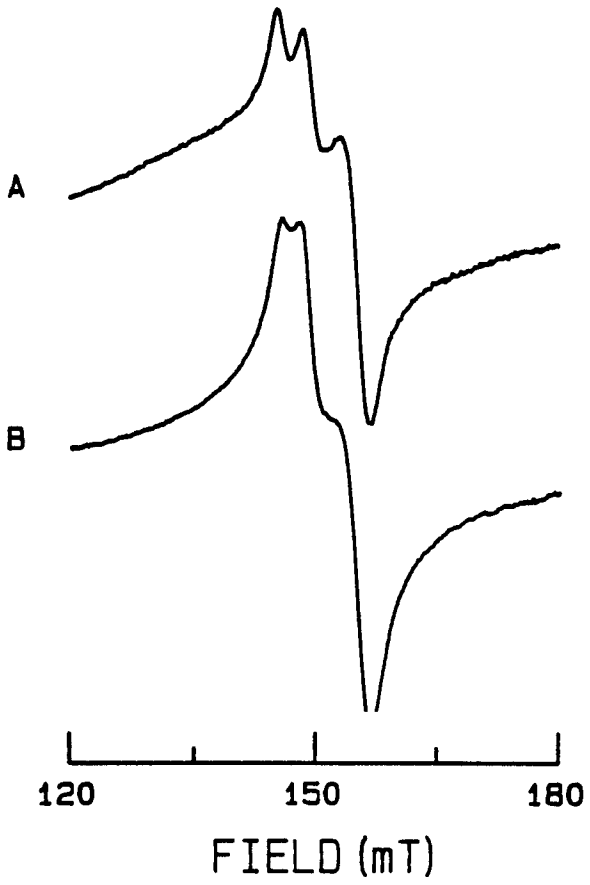

Fig. 2.4 Computer-assisted addition of EPR signals: A. sum of N and C monoferrics with 0.5 M NaCl (compare with Fig. 2.1B); B. sum of N and C monoferrics with 0.5 M $NaClO_4$ (compare with Fig. 2.1C).

TABLE 1

EPR DOUBLET SPLITTINGS[a]

Transferrin Sample	Splitting, mT without $NaClO_4$	Splitting, mT 0.5 m $NaClO_4$	Reduction, mT
Native (pH 7.4)	4.1	2.7	1.4
Native (pH 8.5)	4.0	3.0	1.0
Native (pH 11.2)	3.8	2.9	0.9
Lys modified (pH 7.4)	3.2		
Arg modified (pH 7.4)	3.1		

[a] separation between lines labelled D in Figure 2.1; error ±0.1 mT

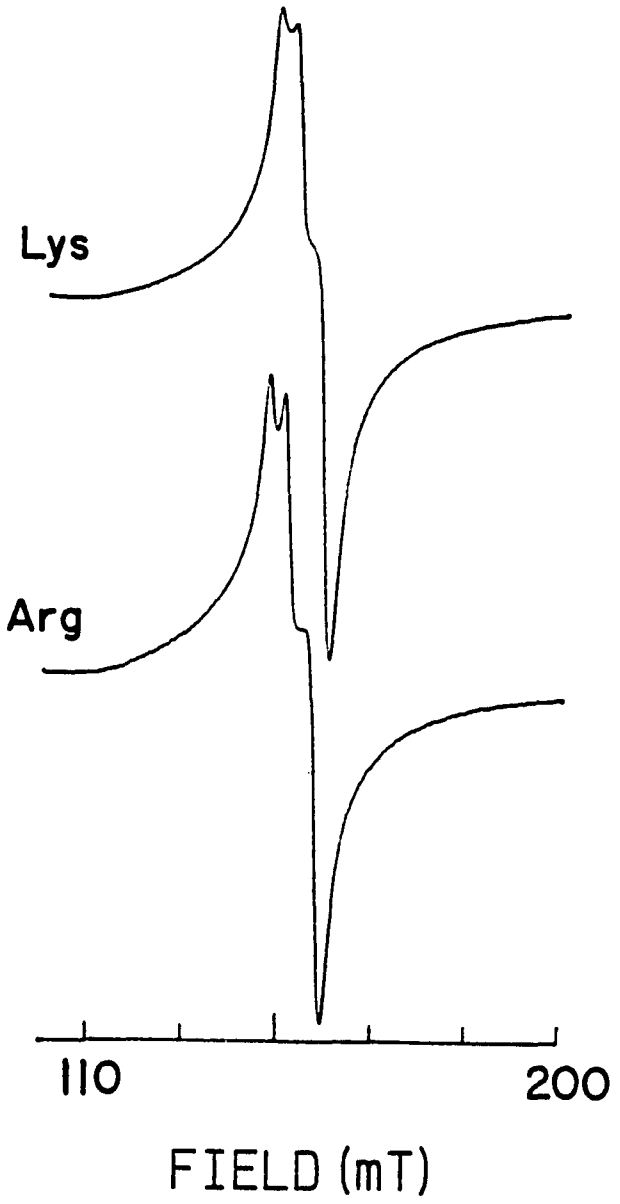

Fig. 2.5 EPR spectra of lysine (83%) and arginine (49.3%) modified transferrins. See Materials and Methods for details. Conditions: 0.3 mM Fe_2Tf in 0.2 M HEPES·Na, 0.015 M $NaHCO_3$, pH 7.4. EPR parameters same as in Fig. 2.1. Spectra scaled to same peak to peak amplitude.

ε-amino groups of lysine and probably guanidinium groups of arginine, whether it be from ClO_4^- binding or chemical modification. Such groups are presumably, but not necessarily, in the vicinity of the metal. As already mentioned, there are several conserved lysine and arginine residues near the proposed locus of iron binding (33). The pair of amino acids Arg-232 and Lys-233 are noteworthy. Figure 2.6 presents an EPR spectral titration of the C-terminal monoferric protein with acetic acid anhydride at constant pH. The coalescence of the doublet at 150 mT is of particular interest.

In Figure 2.6E, where the acetic anhydride to lysine mole ratio equals 26.4, the doublet feature has completely collapsed into a broad singlet. Double integrals and signal amplitudes remain fairly constant throughout the titration (±10%) with the exception of Figure 2.6E, where 59% reduction in double integral and 28% reduction in signal height is observed. This could be due to loss of signal outside of the magnetic field scan range or more likely to loss of EPR observable iron from the C-terminal site. Like perchlorate treatment, lysine modification destabilizes C-terminal transferrin iron. Free iron will quickly hydrolyze and polymerize under these conditions, rendering the iron species EPR silent. Solutions of 1 M acetate, .1 M $NaHCO_3$, and 0.1 mM Fe(III), pH 9, containing no protein have no g' = 4.3 EPR signal.

Perchlorate treatment has already been observed to render the C-terminal site kinetically more labile and the N-terminal iron more inert to removal in pyrophosphate mediated iron release reactions to the terminal iron acceptor, desferrioximine B (24,50). Lysine modification affects the individual sites in a similar way. In Figure

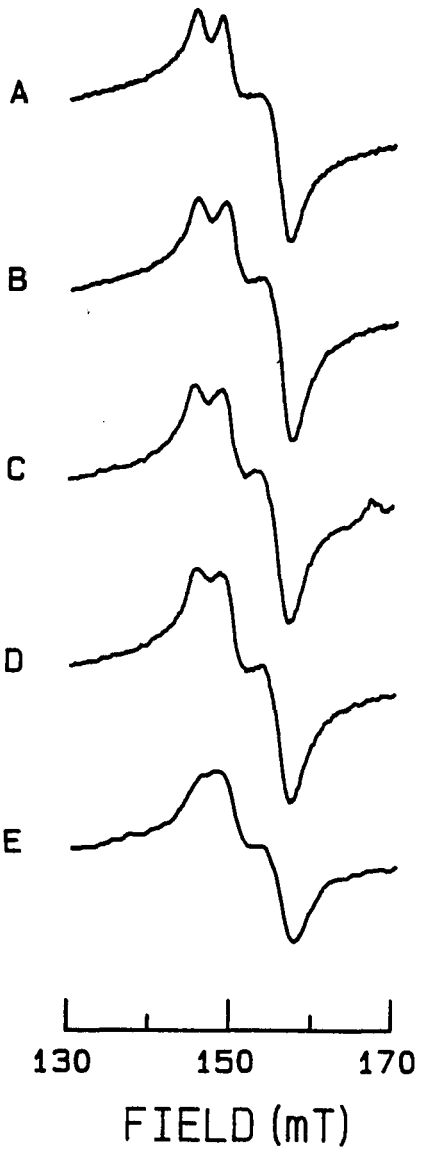

Fig. 2.6 EPR titration of 0.12 mM (in iron) C-terminal monoferric transferrin in 0.1 M $NaHCO_3$ with acetic anhydride, pH 8-9.
A. no acetic anhydride (AA) added, (AA)/(LYS) = 0
B. 3 uL acetic anhydride (AA) added, (AA)/(LYS) = 4.4
C. 6 uL acetic anhydride (AA) added, (AA)/(LYS) = 8.8
D. 12 uL acetic anhydride (AA) added, (AA)/(LYS) = 17.9
E. 18 uL acetic anhydride (AA) added, (AA)/(LYS) = 26.4
EPR parameters: scan rate = 8 min/2000 G, field set = 1500 G, modulation amplitude = 10 G, modulation frequency = 100 kHz, receiver gain = 1000, temperature = 77°K, microwave frequency = 9.14 GHz.

2.7, spectrophotometrically obtained pseudo first-order rate constants for iron release are plotted as a function of lysine modification. A sharp decrease in rate constant breaking at relatively low degrees of acetylation ($\leq$ 15 lysines per mole of protein) for the N-terminal iron and a gradually increasing rate for the C-terminal iron were observed. The coalescence of the EPR spectral doublet as a function of modification appears to be gradual and correlates with the kinetic behavior of the C-terminal iron (Fig. 2.7). From the monitoring of the kinetics and EPR upon modification, it appears that changes in both properties occur simultaneously in the C-terminal domain.

Kinetic data for the citrate mediated C-terminal iron release reaction on unmodified and partially modified samples is listed in Table 2. The unmodified sample has a rate constant of 0.010 min^{-1}. Addition of .5 M perchlorate speeds up the reaction three-fold, as is observed in the pyrophosphate mediated reactions (24). Partial modification of lysines also enhances the rate of C-terminal iron release (0.017 min^{-1}), but the resultant protein is kinetically unresponsive to perchlorate. The results suggest that perchlorate binding to the protein is quenched upon modification of lysines.

Protection Experiments

Due to the tentative assignment of lysine in the perchlorate binding sites of transferrin, we have attempted to protect the protein from modification by using perchlorate. Figures 2.8 and 2.9 show the change in $g' = 4.3$ EPR signals of diferric transferrin upon acetylation in the absence (A) and the presence (B) of 1 M sodium perchlorate. Each sample was then ultrafiltered using an Amicon model 3 cell fitted with a PM 10 membrane to remove reaction products, made 0.2 M in sodium

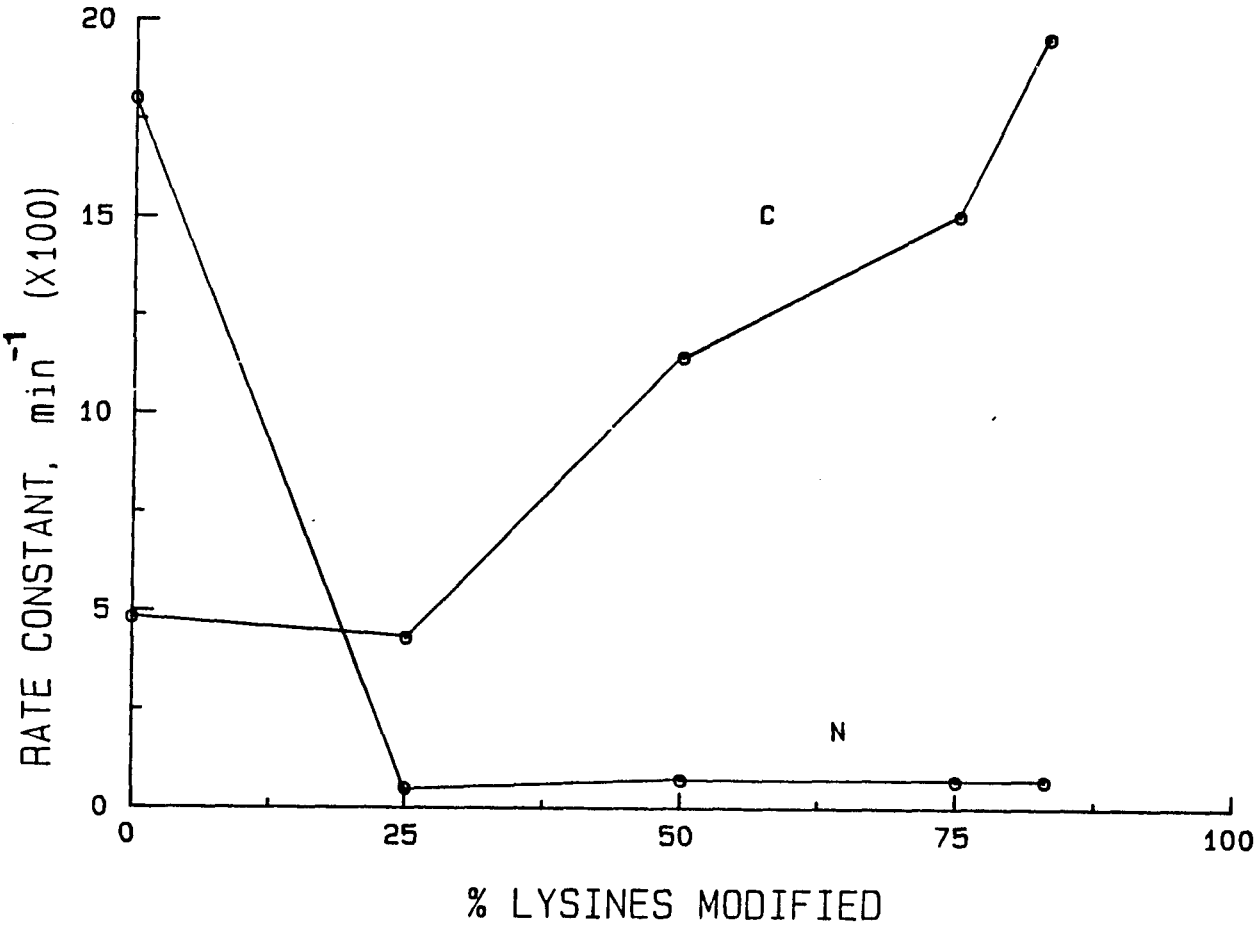

Fig. 2.7 A. Pseudo first-order rate constants for the individual N- and C-terminal iron sites as a function of lysine modification. Conditions for kinetic measurement 2 mM pyrophosphate, 0.9 mM desferal, 0.02 M $NaHCO_3$, T = 37°C, 0.1 M HEPES·Na, pH 6.9.

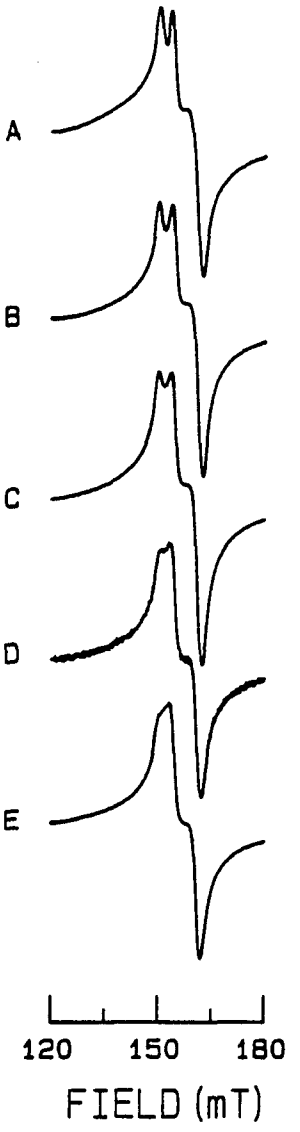

Fig. 2.7 B. g' = 4.3 EPR signal 0.472 mM Fe_2Tf, 83% iron saturated. (A) 0 lysines modified, (B) 25% lysines modified, (C) 50% lysines modified, (D) 75% lysines modified, (E) 83% lysines modified. EPR parameters: scan rate = 8 min/2000 G, field set = 1500 G, time constant = 0.3 sec, modulation amplitude = 10 G, modulation frequency = 100 kHz, receiver gain = 500, temperature = 77°K. Samples are same as in Fig. 2.7A.

TABLE 2

Effect of Acetylation on the Rate of Iron Release From C-terminal Monoferric Transferrin

	Rate Constant (min^{-1})[a]	
Sample	No $NaClO_4$	0.5 M $NaClO_4$
C-terminal (control)	0.010	0.033
C-terminal (25% LYS MOD)	0.017	0.017
C-terminal[b] (38% LYS MOD)	0.023	0.014

[a]Iron release reaction performed in 5.0 mM sodium citrate and 1.4 mM desferal. All other conditions as in Materials and Methods.

[b]Modification reaction performed in the presence of 0.5 M $NaClO_4$.

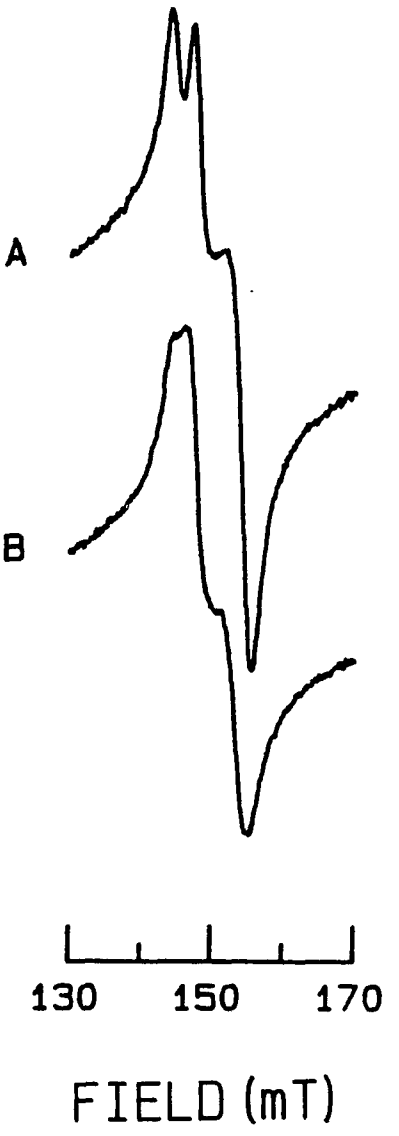

Fig. 2.8 A. g' = 4.3 EPR signal of 0.10 mM diferric transferrin, pH 9.1 in 0.02 M $NaHCO_3$ at 108°K. Instrument settings: power = 20 mW, scan time = 8 min/2000 G, field set = 1500 G, time constant = 0.3 sec, modulation amplitude = 10 G, modulation frequency = 100 kHz, receiver gain = 2000, microwave frequency = 9.100 GHz.

B. g' = 4.3 EPR signal of .10 mM diferric transferrin, pH 9.1 in 0.1 M $NaHCO_3$/1 M $NaCLO_4$. Instrument settings same as in Fig. 2.8A.

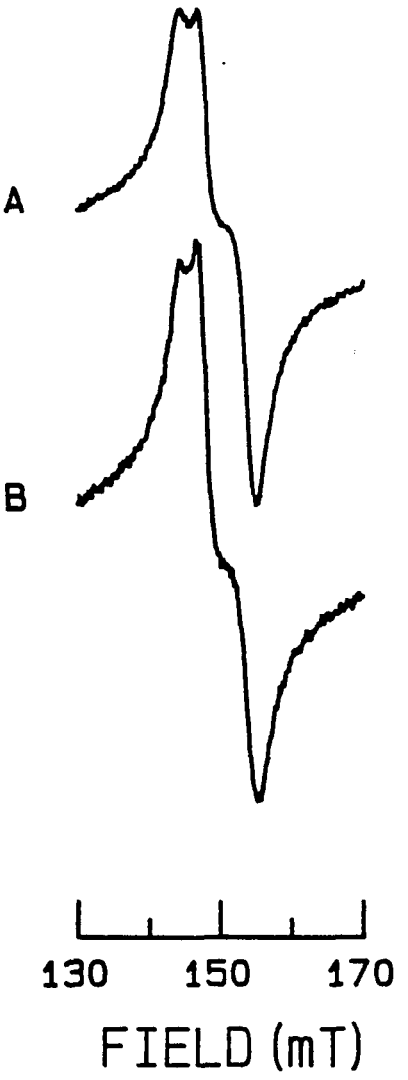

Figure 2.9 A. g' = 4.3 EPR signal of 0.10 mM diferric transferrin, 63% lysine modified, by adding 6 uL acetic anhydride + 200 uL 1 M NaOH to 2 mL of sample shown in Figure 2.8A. All EPR parameters same as in Fig. 2.8A.

B. g' = 4.3 EPR signal of 0.10 mM diferric transferrin, 83% lysine modified, by adding 6 uL acetic ahydride + 285 uL 1 M NaOH to 2 mL of sample shown in Fig. 2.8B. All conditions and EPR parameters same as in Fig. 2.8A.

perchlorate and the EPR spectra monitored at each step (Figs. 2.10 and 2.11). The reduction in EPR signal, characteristic of the perchlorate effect is quantitated and used as a measure of perchlorate binding to the protein.

When 2 mLs of 0.1 mM diferric transferrin in 0.1 M $NaHCO_3$ was treated with 6 uL of acetic acid anhydride, 63% of the lysines were acetylated. The double integral of the EPR signal was reduced by 25%, indicating possible loss of iron from the protein. The subsequently ultrafiltered sample exhibits a reduction in EPR signal amplitude of 28.4% (Fig. 2.10) upon addition of perchlorate. In the presence of 1 M sodium perchlorate, otherwise identical acetylation conditions effects modification of 83% of the lysines. The double integral of the EPR signal was reduced by 50%. This observation suggests that about half of the iron is being lost from the protein. After ultrafiltration, this sample shows a reduction in EPR amplitude of only 9.4% upon perchlorate addition (Fig. 2.11).

The data in Figures 2.10 and 2.11 seem to indicate that the presence of perchlorate during the modification step somehow quenches the subsequently measured EPR "perchlorate effect", as evidenced by EPR signal height reductions. However, based on the above data, another interpretation is offered. The combination of perchlorate and acetylation probably removes iron from the C-terminal site of the protein. This speculation is in accord with the data in Table 2 that shows that both perchlorate and acetylation separately render C-terminal iron less stable toward citrate mediated release to desferrioximine B. The removal of iron from one site is also consistent with the observed 50% reduction in double integral and

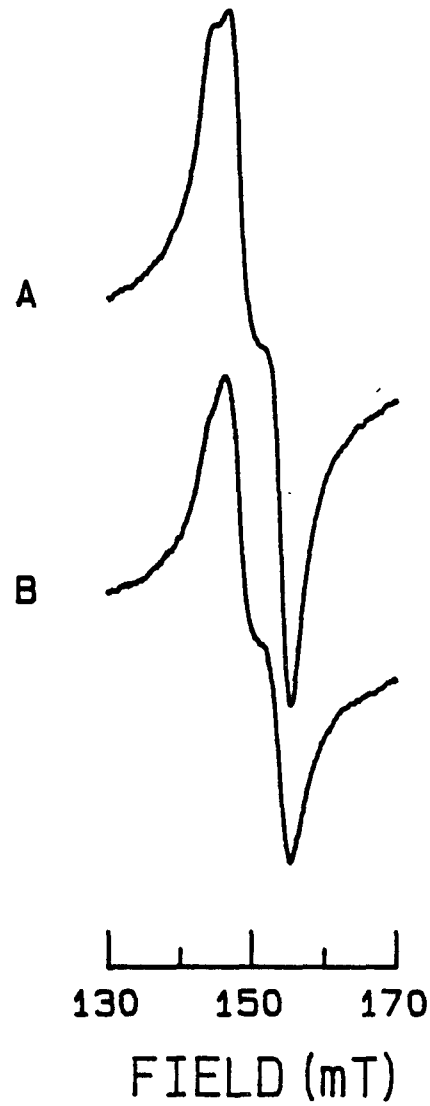

Figure 2.10 A. g' = 4.3 EPR signal of modified sample shown in Fig. 2.9A after ultrafiltration 3 times against 0.1 M $NaHCO_3$ (see Materials and Methods). All conditions and EPR parameters same as in Fig. 2.8A.

B. g' = 4.3 EPR signal of modified protein sample shown in Figure 2.10A after addition of 0.2 M sodium perchlorate. All other conditions and EPR parameters same as in Fig. 2.8A.

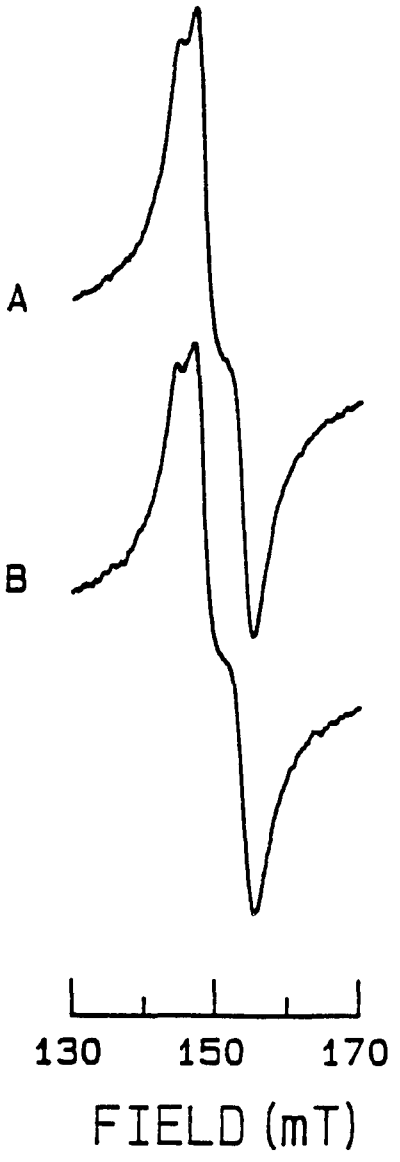

Figure 2.11 A. g' = 4.3 EPR signal of modified protein sample shown in Fig. 2.9B after ultrafiltration (see Materials and Methods). All conditions and EPR parameters same as in Fig. 2.8A except receiver gain is 3200.

B. g' = 4.3 EPR signal of modified protein sample shown in Fig. 2.11A after addition of 0.2 M sodium perchlorate. All conditions and EPR parameters same as in Fig. 2.11A.

higher extent of modification when perchlorate is present during acetylation. When transferrin releases its iron, the protein unfolds, thus exposing more groups for modification.

In lieu of the above arguments, the protection experiments were deemed unsuccessful. Further experiments using thiocyanate as a "protector" anion in place of perchlorate were also unsuccessful for similar reasons. Finally, protection experiments with the C-terminal monoferric protein were attempted, but iron scrambling between the two binding sites was a problem. Future work in this area might be more fruitful if a protecting anion that binds tightly to the protein, yet does not remove iron, is employed. Bulky sodium dodecyl sulfate might prove useful.

DISCUSSION

The three component g' = 4.3 EPR signal is characteristic of iron-transferrin complexes (51). Other iron-protein or iron-chelate complexes do not exhibit such a signal. The detailed theoretical origins of this signal are not well understood. In model iron compounds of pure rhombic symmetry, the g' = 4.3 EPR signals are structureless in theory and practice. The signal arising from transferrin iron has never successfully been simulated using a single spin Hamiltonian. The difficulty is due primarily to the lack of exact reproduction of the doublet feature and tailoring of EPR amplitude into the wings.

The transferrin signal may arise from the contributions of two protein conformations in equilibrium. By assuming two iron geometries, the transferrin signal, including its unique doublet, can be simulated (51). Guinea pig transferrin, which does not possess a doublet feature in its g' = 4.3 EPR signal, can be simulated using a single hamiltonian spin operator, suggesting one iron-ligand geometry. The C-terminal iron might also be cast into a single ligand conformation by either lysine modification or perchlorate treatment. Either method causes coalesence of the g' = 4.3 signal into a broad singlet.

The loss in resolution and amplitude of the EPR signal has been suggested to occur through local conformational changes effected by perchlorate (24,30-32). By quantitation of the transferrin spectral changes that develop in a perchlorate titration, specific anion binding

to the protein has been demonstrated (32a). Very little is known about the nature of these perchlorate binding sites and their proximity to the metal. Although the possibility exists that perchlorate binds at sites some distance from the metal, there is evidence that binding occurs close to the metal site. Feeney and co-workers have observed that the transferrin phenolate metal ligands of apotransferrin are highly reactive toward periodate oxidation (52). They suggest that the tyrosine ligands are located in a region of high positive charge on the protein, thus directing the periodate reaction. Periodate and perchlorate are isostructural.

The amino acid string model of the proposed transferrin metal binding site shows the presence of several lysines and arginines in the vicinity of the probable metal ligands (33). Such a model aided in the identification of a single histidine residue, associated with the in vitro mechanism of transferrin iron removal (Chapter 1). The kinetic data (Fig. 2.7) indicates that the modification of a small number (< 15) of fairly reactive lysine residues in the N-terminal domain correlates with the observed retardation of iron removal. Similarly, the modification of a small number of lysines may be responsible for the observed loss of EPR spectral resolution (Fig. 2.6) and iron lability (Fig. 2.7) in the C-domain.

Evidence is growing that the chemical properties of transferrin iron are strongly influenced by local protein conformations. Sequence analysis (14) shows that several carboxyl groups are located in the vicinity of the probable metal binding sites and especially in the N-terminal domain. Baldwin and co-workers have shown that lithium salts also influence the kinetics of transferrin iron (24). Bezkorovainy

and co-workers found that the iron binding activity of one site in apotransferrin is lost upon extensive carboxyl group modification (54).

In the present study, evidence is provided that is consistent with the hypothesis that perchlorate binds to a richly cationic region of the protein, possibly near to the metal. An ensuing conformational change occurs which alters the kinetic and spectral properties of the transferrin iron. Further work must be done to understand the observed differential kinetic effect of lysine and arginine modification and perchlorate addition at the two sites and to better characterize these important anion binding sites.

CHAPTER III

STUDY OF IRON-ATP INTERACTIONS

INTRODUCTION

The question of whether ATP and iron-ATP complexes play an important biological role in iron metabolism is an important one. Such complexes are of particular interest since they could easily form *in vivo* and may participate in intracellular iron transport and deposition in ferritin. In a 1981 report, Crichton followed the *in vitro* transfer of iron (as ^{59}Fe) from transferrin to ferritin, in the presence of ATP. He found that ATP can mediate release of iron from transferrin to form a stable Fe(III)-ATP complex at pH 7.4, which subsequently facilitates iron deposition into ferritin (21).

In 1964, Goucher and Taylor first investigated the existence and composition of some ferric nucleotide phosphates (58). The apparent formation constants of 1:1 complexes of iron and several nucleotides were reported. Since then little attention has been paid to the reactions between iron and purine nucleotides. In 1976, Bartlett (20) isolated small and variable amounts of ferric-ATP from the cytosol of red blood cells and identified it to be the 1:1 complex studied by Goucher and Taylor.

In the present study, a combination of chemical and spectroscopic methods used to show that both mononuclear and polynuclear Fe(III)-ATP complexes readily form in solution at physiological pH, depending on the Fe:ATP ratio. Mononuclear Fe(III) was stabilized by excess ATP (Fe:ATP < 1:3). Polynuclear species, formed at an Fe:ATP ratio of 4:1, consisting of a cluster of 250 or more iron atoms with the approximate formula $[Fe(OH)_{2.5}^{+.5}]_4 \cdot ATP$.

MATERIALS AND METHODS

$Fe(NO_3)_3 \cdot 9H_2O$ was obtained from Baker Chemical Co., Hepes buffer from Research Organics, ribose 5-phosphate from Boehringer Mannheim, 2'-deoxyadenosine triphosphate from P-L Biochemicals, Inc., and Pentex horse spleen ferritin from Miles Laboratories. All other materials were Sigma products and used without further purification. ATP solutions were standardized spectrophotometrically, using $\varepsilon = 15.4 \times 10^3\ M^{-1}cm^{-1}$ at 259 nm (65). Fe(III)-ATP complexes were formed by the slow addition of a commerical 0.179 M $FeCl_3$ standard solution in 1 M HCl to 3.3 mM ATP in 0.1 M HEPES·Na buffer, pH 7.0, with stirring using 1.00 N NaOH to maintain the pH. In experiments to quantitate the number of protons released upon Fe(III)-ATP cluster formation, a freshly prepared aqueous solution of 0.150 M $Fe(NO_3)_3$, standardized by the thiocyanate method (59), was added to 6.2 mM ATP in 0.1 M HEPES·Na buffer, pH 7 or 9, until an Fe:ATP ratio of 4:1 was obtained. The total amount of 1.00 N NaOH required to maintain the pH was recorded. The free acid in the ferric nitrate solution was shown to be negligible by addition of an equimolar amount of Na_2EDTA to complex the iron, followed by potentiometric titration with two equivalents of 1.00 N NaOH to its end point. pH was measured with a Radiometer model PHM26 pH meter equipped with a Radiometer GK2321C glass/Ag-AgCl combination electrode. Ultrafiltration or dialysis experiments were carried out with Amicon membranes having molecular weight exclusion sizes of 500 (UM05), 10,000 (PM10), 30,000 (PM30), and 50,000 (XM50), and with

Spectrapor type 6 dialysis tubing having a molecular weight exclusion size of 2,000.

Electron paramagnetic resonance spectra of samples in calibrated EPR tubes were measured at 77° K on a Varian E-4 spectrometer employing a TE_{102} rectangular cavity and a dewar insert. Spectra were acquired on a Digital Equipment Corporation MINC-23 laboratory computer and double integrated to determine spin concentrations. $FeEDTA^-$ (0.1 M EDTA, 1 mM Fe^{3+}, pH 7.8) was used as an intensity standard for the $g' = 4.3$ signal and 0.5 mM $CuSO_4$, 0.2 M HCl in glycerin/H_2O 1:3 for the $g' = 2$ signal. Infrared spectra of lyophilized 4:1 Fe(III)-ATP samples in KBr pellets were measured on a Perkin Elmer 283B infrared spectrophotometer, and optical spectra of solutions measured on a Cary 219A dual beam recording spectrophotometer. The brown lyophilized samples re-dissolved in water to form the characteristic reddish brown solution of the cluster. ^{31}P NMR spin-lattice relaxation times were determined by the inversion recovery method (19) using a JEOL FX90Q spectrometer operating at 36.2 MHz for phosphorus-31.

RESULTS

Figure 3.1 (inset) shows the g' = 4.3 EPR signal of a solution of 0.79 mM Fe(+3) in 3.39 mM ATP, buffered at pH 7 with 0.10 M Hepes·Na. The signal arises from high spin Fe(+3) in a coordination environment of rhombic symmetry (51). Figure 3.1 shows an EPR spectral titration of ATP with Fe(+3), delivered as $FeCl_3$ in 1 M HCl. The titration curve shows a linear rise in signal intensity, breaking at an Fe:ATP mole ratio of 1:3. Up to this point in the titration, all of the added iron can be accounted for by the EPR spectrum as determined by a comparison of the double integrals of this signal with the signals from $Fe(EDTA)^{-1}$ standards. Therefore, to the precision (±15%) of the spin concentration measurement, all of the iron before the 1:3 break is in the form of a mononuclear species. Beyond the 1:3 ratio the reduction in EPR intensity is indicative of the presence of polynuclear iron species. Further discontinuities in the curve occur at 2:1 and 4:1. At the latter break point, only g' = 4.3 EPR silent species exist. Figure 3.2 shows the UV-Vis spectra of free ATP and the 4:1 Fe:ATP cluster.

To further examine the mononuclear Fe-ATP complexes, ^{31}P NMR spectroscopy was undertaken. The resonances of the α, β, and γ phosphorus nuclei of 0.1 M ATP were visibly unchanged by the presence of 100 uM Fe(+3) at pH 7.0. However, the presence of paramagnetic iron enhances the spin-lattice relaxation rates ($1/T_1$) of the ^{31}P nuclei, as shown in Figure 3.3. This is consistent with iron coordination through the oxygen atoms of the phosphate groups of ATP.

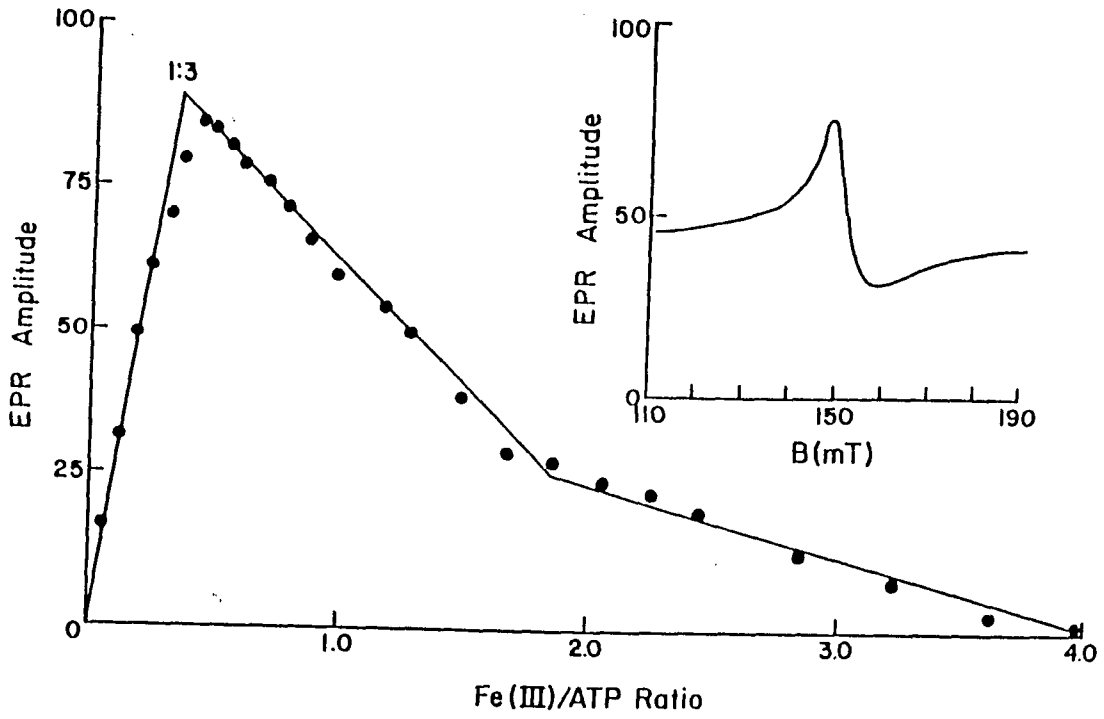

Fig. 3.1 Dependence of the amplitude of the g' = 4.3 EPR signal (inset) on the Fe(III)/ATP mole ratio. Species formed at Fe:ATP ratios of 1:3, 2:1, and 4:1 are indicated. Conditions: Fe(III) added as 0.179 M $FeCl_3$ in 1 M HCl to 3.39 mM ATP in 0.1 M HEPES·Na buffer, pH 7, maintained with 1 M NaOH. EPR instrument settings: field set = 1500 G, scan range = 2000 G, microwave power = 20 mW, klystron frequency = 9.145 GHZ, modulation amplitude = 10 G, modulation frequency = 100 kHZ, receiver gain = 1000, scan time = 8 min, time constant = 0.30.

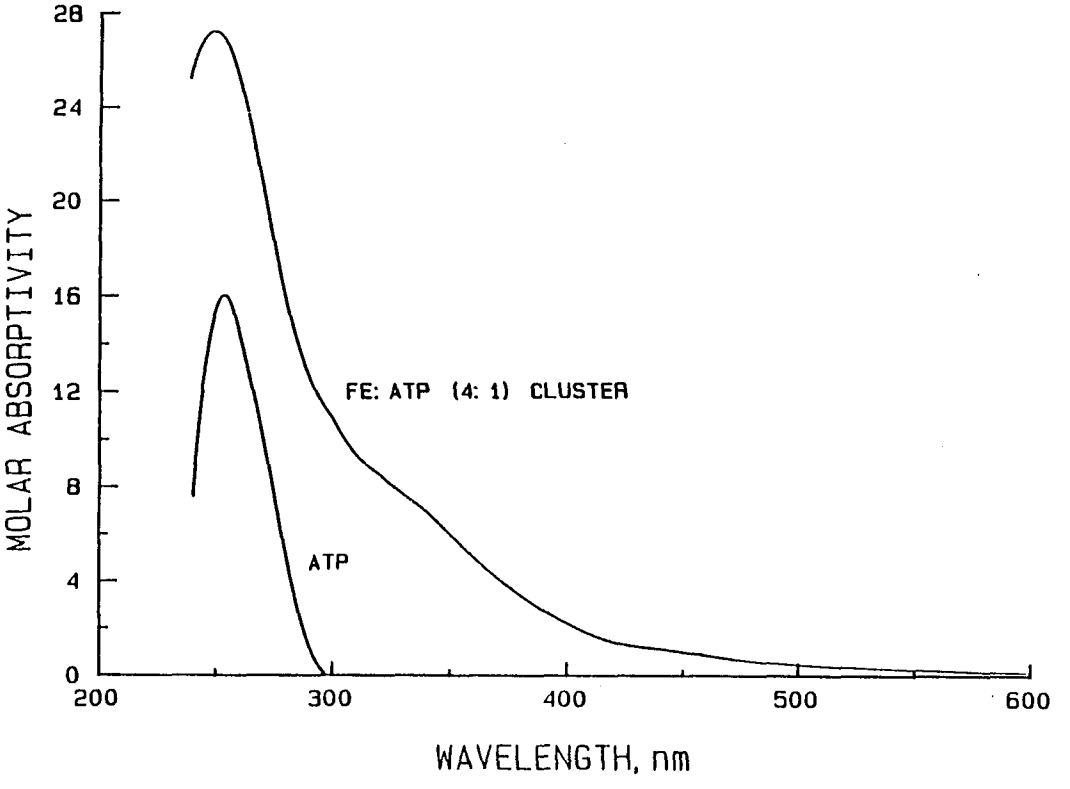

Fig. 3.2 UV-Vis spectrum of ATP and the Fe:ATP (4:1) cluster.

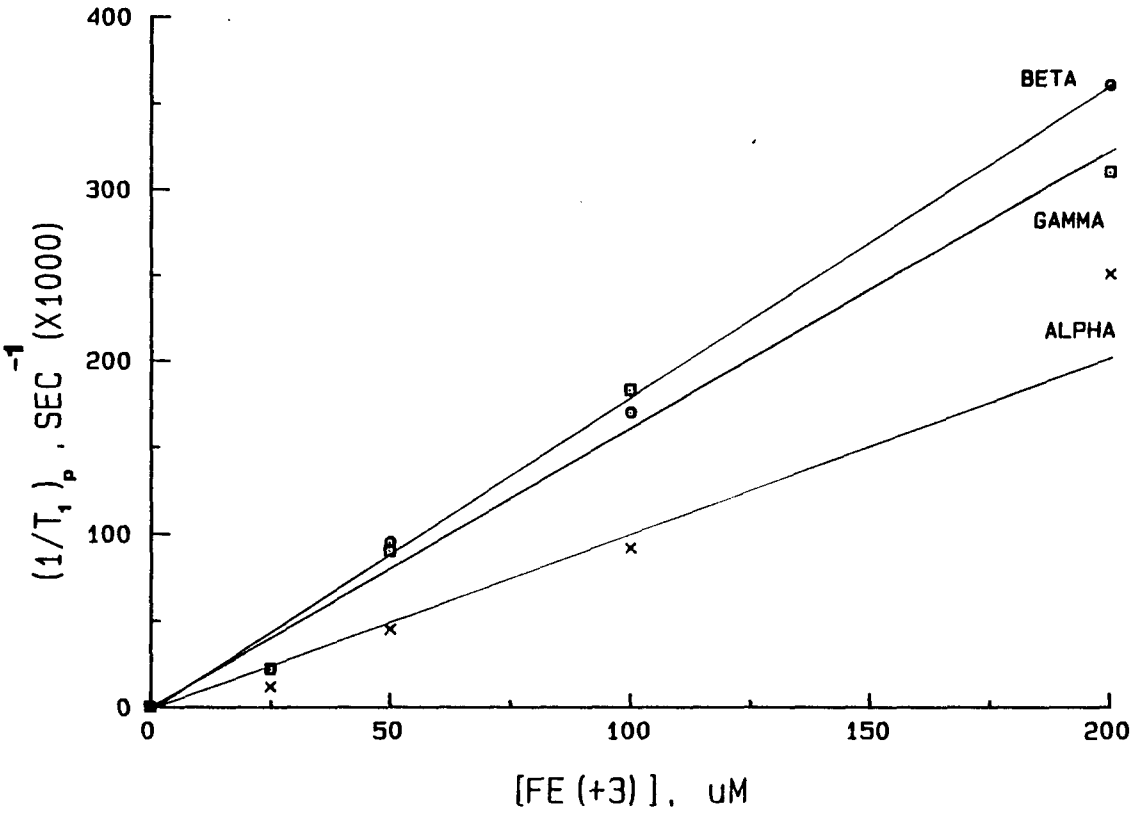

Fig. 3.3 Paramagnetic contribution $(1/T_1)_p$ of spin-lattice relaxation rate for α, β, and γ phoshorus nuclei of ATP as a function of iron concentration. Conditions: Fe^{+3} added as $FeCl_3$ in acid, [ATP] = 0.1 M in 0.1 M HEPES·Na, pH 7, previously chelexed and dialyzed against APO transferrin to remove trace amounts of iron in solution. See Materials and Methods.

The net magnitude of the paramagnetic enhancement $(1/T_1)_P$ values (Fig. 3.3) indicate that the paramagnetic contribution to the relaxation rate is dominated by the Γ_M value, the residence time of the ATP in the first coordination sphere of the Fe(III). From the data in Figure 3.3, Γ_M values of the α, β, and γ ^{31}P nuclei of 11, 5.8, and 5.4 ms., respectively, were obtained at 28°C.

Weak ^{31}P NMR signals in the Fe(III):ATP (4:1) complex were observed and attributed to trace amounts (~ 1%) of ADP and P_i. The lack of an ATP NMR spectrum is presumably due to paramagnetic broadening of the NMR lines. Fe(III) does not bind strongly to ADP, as reported previously (58). Solutions of the Fe(III):ATP (4:1) complex did, however, exhibit a broad EPR signal centered at g' = 2.0, having a line width of Δ Hpp ~ 1000 G. Quantitative spin determination of this signal indicates that only 0.8% of the iron present contributed to this signal if it arises from an S = 5/2 spin state and 9.3% if it arises from an S = 1/2 spin state. The major portion exists as an EPR silent species, consistent with other known polynuclear Fe(III) species.

The approximate molecular weight of the Fe(III):ATP (4:1) cluster was estimated using ultrafiltration membranes and dialysis tubing of varying molecular weight cutoff values. Iron was nearly completely retained by ultrafiltration membranes with exclusion limits of ~ 10,000 molecular weight. However, 18 $\pm$ 2% of the iron passed through a membrane that retains molecules of approximately 50,000 MW. From these observations it was concluded that most of the iron, although polydisperse in size, is in the form of a polynuclear cluster of greater than 50,000 MW. Such a cluster would contain 250 or more iron atoms.

Proton release experiments, as Fe(III) was added to ATP at pH 7 and pH 9, were performed. A value of 2.5 ± .1 H^+ released per metal was obtained, suggesting an empirical formula of $Fe(III)(OH)_{2.5}^{+.5}$, in agreement with the composition of other known polynuclear iron complexes (60).

Attempts were made to identify specific donor groups which stabilize the 4:1 ligand to metal cluster. Solutions of 2'-deoxyadenosine triphosphate (2'dATP), tripolyphosphate (TP), pyrophosphate (PP_i), orthophosphate (P_i), adenosine 5'-monophosphate (AMP), and ribose 5'-phosphate (R 5'-P) were individually tested at iron to ligand ratios of 2:1 and 4:1. None formed soluble complexes with the exception of 2'dATP (Fig. 3.4). The tripolyphosphate titration is shown in Figure 3.5, where a 1:2 (Fe:TP) break is observed. In order to establish the necessity of the adenine ring in Fe:ATP (4:1) cluster formation, sister experiments were done using equimolar amounts of PP_i and AMP or R 5'-P. The former solution readily solubilized four moles of Fe(III) to form a deep brownish red solution, characteristic of the Fe(III):ATP (4:1) cluster. The R 5'-P/PP_i solution, which lacks only the adenine ring, solubilized four moles of Fe(III) only when the iron solution was added slowly over a 48 hour period. These results suggest a role of adenine in the facilitation of iron-ATP cluster formation.

Infrared spectra of the polynuclear Fe(III):ATP (4:1) complex and ATP (67) showed that iron complexation caused a decreased intensity in the P-O stretch at 1250 cm^{-1} and a shift in the 1700 cm^{-1} bending mode of the $-NH_2$ group of adenine to 1650 cm^{-1} (Fig. 3.6), suggesting involvement of both of these groups in iron binding. Coordination through the 3' oxygen of the ribose moiety of ATP was not excluded.

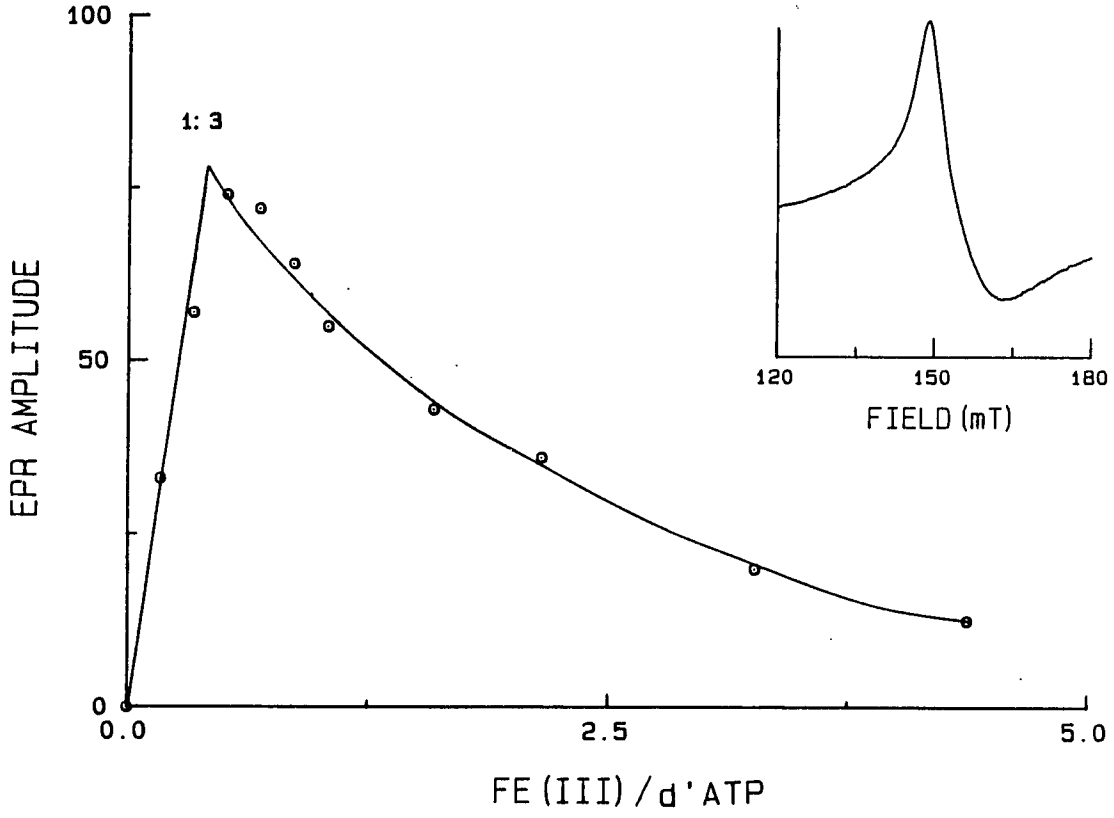

Fig. 3.4 Dependence of the amplitude of the g' = 4.3 EPR signal (inset) on the Fe(III)/3'dATP mole ratio. Conditions: Fe(III) added as 0.15 M $Fe(NO_3)_3$ in HCl to 3.24 mM 3'dATP. All other conditions and instrumental settings same as in Fig. 3.1.

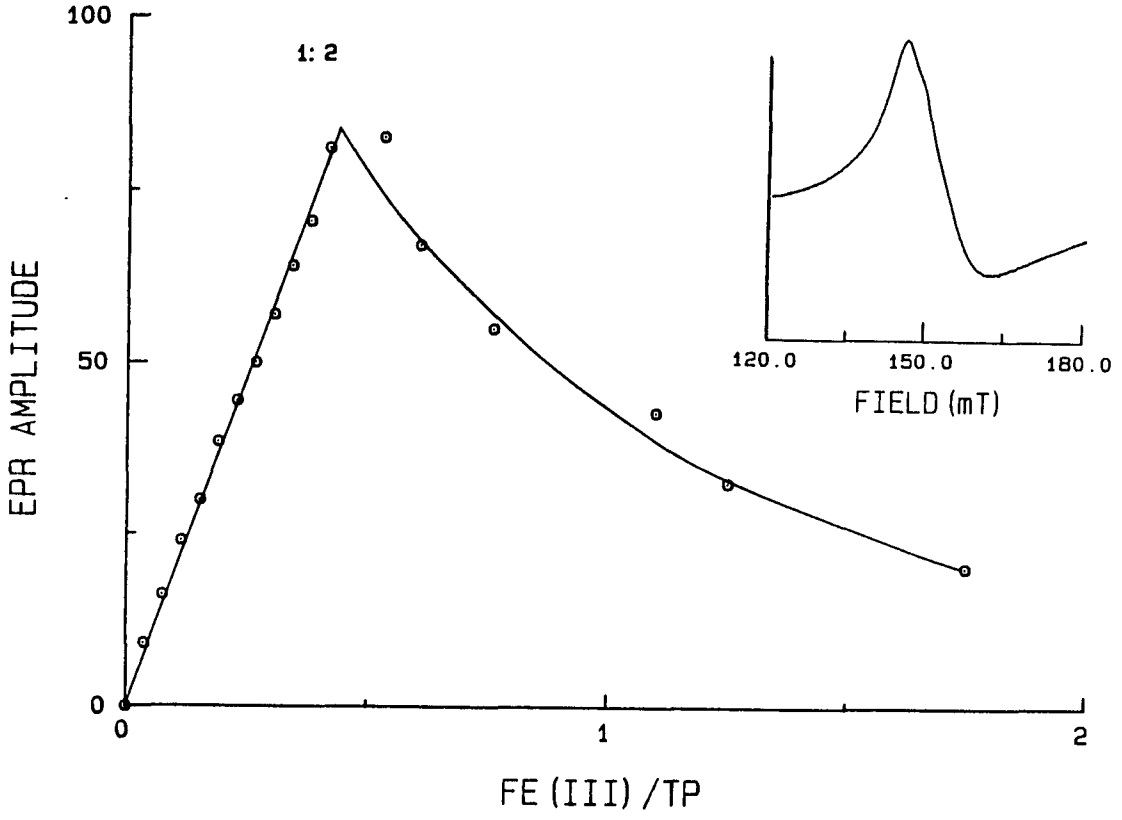

Fig. 3.5 Dependence of the amplitude of the g' = 4.3 EPR signal (inset) on the Fe(III)/TP mole ratio where TP = tripolyphosphate. Conditions: Fe(III) added as 0.18 M $Fe(NO_3)_3$ in HCl to 7.33 mM TP in 0.1 M HEPES·Na, pH 7, maintained with 1 M NaOH. EPR settings same as in Fig. 3.1 except RG = 200.

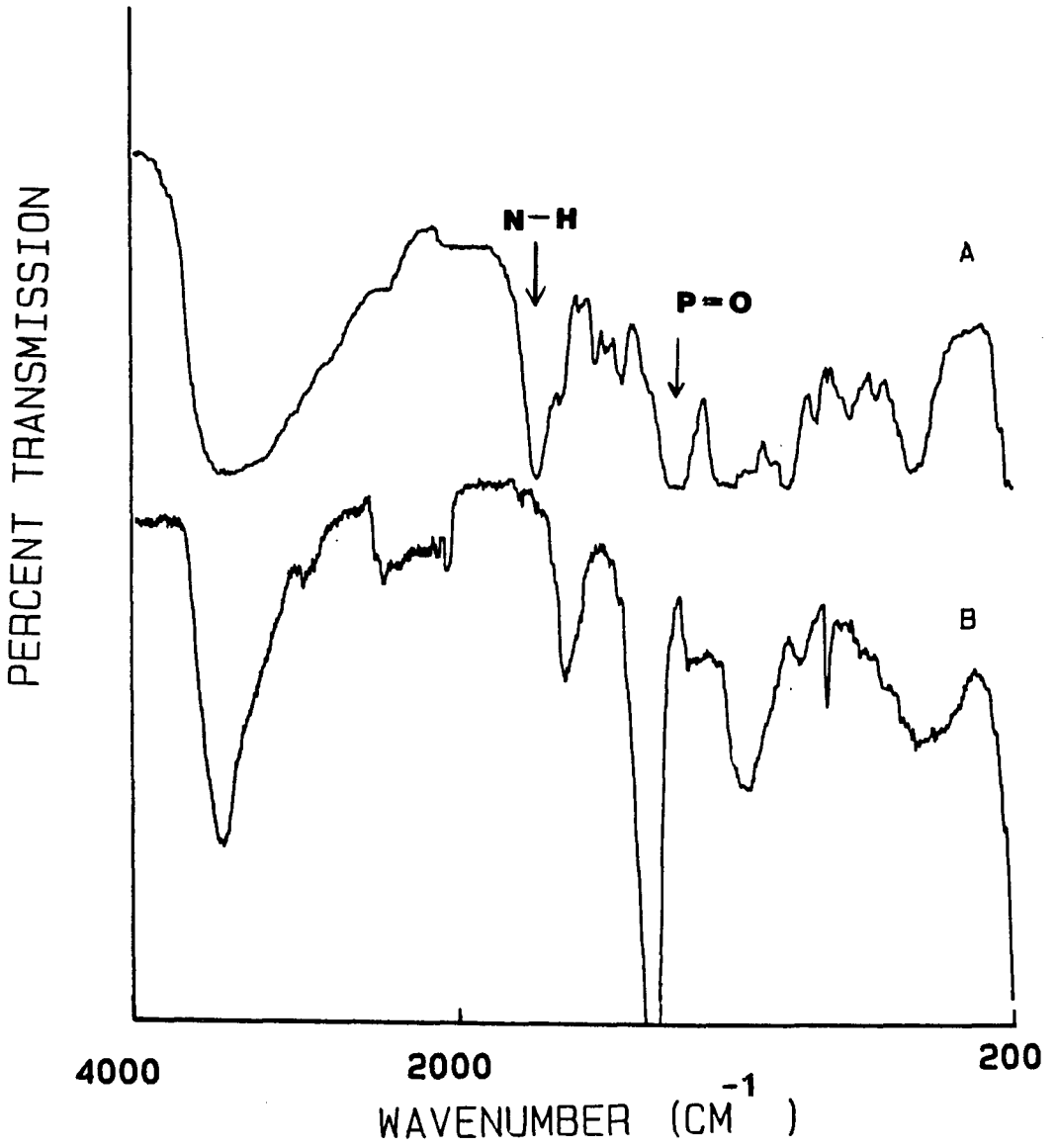

Fig. 3.6 Infrared spectra of polynuclear Fe(III):ATP (4:1) complex (A) and free ATP (B). See Materials and Methods for details.

DISCUSSION

Complexes between adenine nucleotides and Fe(III) at physiological pH have not been studied much. The 1:1 complexes between Fe(III) and ATP (58) or AMP (61) are formed by precipitation at pH 2. Bartlett reported 1:1 Fe:ATP complexes at neutral pH. In the present study we demonstrated that at least three different types of complexes were formed between Fe(III) and ATP at neutral pH, as evidenced by discontinuities in the EPR titration curve (Fig. 3.1) at Fe:ATP ratios of 1:3, 2:1, and 4:1. Of these, only the first complex appeared to be mononuclear and gave rise to a g' = 4.3 EPR signal.

It is difficult to identify the coordinating phosphate groups in the 1:3 (Fe:ATP) complex since the spin-lattice relaxation times of all three phosphorus nuclei are affected by the presence of Fe(III). The similarity in the Γ_M values for the β and γ nuclei suggests that bidentate coordination occurs through these groups. The observed stoichiometry of 1:3 (metal:ligand) is also consistent with bidentate coordination. The similarity between the g' = 4.3 EPR signal of Fe-2'dATP and Fe-ATP is suggestive of similar iron environments. This would preclude the 2'-hydroxyl group on the ribose moiety as a possible donating group in $Fe(ATP)_3$ solutions.

Although ATP interactions with Fe(III) have not been studied much, there are several reports of ATP interactions with other transition metals. In these studies ^{31}P NMR measurements were useful in identifying the coordinating phosphates of ATP with manganese (62), aluminum (63), and vanadyl (64). It is noteworthy that the Γ_M of

Fe(III)-ATP is approximately 10 times smaller than that of Al(III)-ATP and 1000 times smaller than that of Mn(II)-ATP. Thus the ligand exchange rate is considerably slower in the iron complex compared to the other metal ions, a result consistent with the known lability of the inorganic complexes of these metal ions.

The Fe(III):ATP (4:1) cluster, having an empirical molecular formula of $[Fe(OH)_{2.5}^{+.5}]_4ATP$ and a minimum molecular weight of ~ 50,000 (> 250 Fe(III) atoms per cluster) appears to follow typical hydrolysis chemistry for Fe(III). Anionic chelators such as citrate or carboxylate groups in dextran have been shown to provide the necessary charge stabilization in such polynuclear iron-oxy clusters; presumably phosphate plays such a role in the Fe:ATP (4:1) cluster.

Polynuclear iron complexes of hydrolyzed Fe(III) phosphate also occur in cells where the iron core of ferritin contains up to 4500 Fe(III) atoms (68). Ferritin and the Fe:ATP (4:1) cluster described here are very similar in appearance, a deep brownish red. Optical measurements at 420 nm indicate a molar absorptivity per iron of 322 $M^{-1}cm^{-1}$ for the solution of the polynuclear Fe(III)-ATP (4:1) cluster (Fig. 3.5), which is close to the value of 362 $M^{-1}cm^{-1}$ for a ferritin sample containing an average of 1400 Fe(III) atoms per protein molecule.

EXAFS analysis of the polynuclear Fe(III)-ATP complex, performed by Drs. Theil and Sayers of North Carolina State University in collaboration with this laboratory, was able to distinguish an Fe-P distance of 3.27 Å, an Fe-O distance at 1.95 Å, and an Fe-Fe distance of 3.36 Å (63). The latter two are the same as in the protein, ferritin. The Fe-P distance is analogous to that in other metal-ATP

complexes (62). The ability of EXAFS to distinguish an Fe-P distance requires at least 70% of the iron to be coordinated to ATP. For this requirement to be met, the ATP must be distributed throughout the cluster. This observation is unique. Previously, polynuclear iron clusters have been thought to be stabilized primarily by surface interactions with anions (60,66).

In conclusion, the existence of Fe(III)-ATP complexes at physiological pH suggests that such complexes could exist *in vivo* and, following iron dissociation from transferrin, may provide a means for intracellular iron transport and deposition into ferritin. In addition, stable Fe(III) complexes may contribute to iron toxicity by altering the size of the nucleotide pool in situations of iron overload.

LIST OF REFERENCES

1. Pollycove, M. In The Metabolic Basis of Inherited Disease, 2nd ed. (1966). McGraw Hill, NY, p. 780.

2. Crichton, R.R. Struct. Bond. (1973) 17, 63.

3. Feeney, R.E. and S.K. Komatsu. Struct. Bond. (1966) 1, 149.

4. Chasteen, N.D. Coord. Chem. Rev. (1977) 22, 1-36.

5. Aisen, P. and I. Listowski. Ann. Rev. Biochem. (1980) 49, 357.

6. Morgan, E.H. Mol. Asp. Med. (1981) 4, 1.

7. Chasteen, N.D. In Iron Binding Proteins Without Cofactors or Sulfur Clusters (Theil, E.C., G.I. Eichorn, and L.G. Marzilli, eds.). Adv. Inorg. Biochem., Vol. 5, (1983) Elsevier, NY, pp. 202-235.

8. Bezkorovainy, A. and D. Grohlich. Biochim. Biophys. Acta (1976) 426, 385.

9. Luk, C.K. Biochemistry (1971) 10, 2838.

10. Rogers, J.B., R.A. Gold, and R.E. Feeney. Biochemistry (1977) 16, 2299.

11. Mazurier, J., D. Luger, V. Tordera, J. Montrevil, and G. Spik. Eur. J. Biochem. (1981) 119, 537.

12. Rogers, T.B., T. Borresen, and R.E. Feeney. Biochemistry (1978) 17, 1105.

13. Buttkus, H., J.R. Clark, and R.E. Feeney. Biochemistry (1965) 4, 998.

14. MacGilliuray, R.T.A., E. Mendez, S.K. Sinha, M.P. Sutton, J. Lineback-Zins, and K. Brew. Proc. Natl. Acad. Sci., USA (1982) 79, 2504.

15. Williams, J., T.C. Elleman, I.B. Kingston, A.G. Wilkins, and K.A. Kuhn. Eur. J. Biochem. (1982) 122, 297.

16 Williams, J. Trends Biochem. Sci. (1982) 1, 394.

17. Aisen, P., A. Leibman, and J.L. Zweier. J. Biol. Chem. (1978) 253, 1930

18. Morgan, E.H. Med. J. Aust. (1972) 2, 322.

19. Fletcher, J. and E.R. Huehns. Nature (1968) 218, 1211.

20. Bartlett, G.R. Biochim. Biophys. Acta (1976) 70, 1063.

21. Konopka, K., J.-C. Mareschal, and R.R. Crichton. Biochim. and Biophys. Acta (1981) 677, 417.

22. Harris, D.C. Biochemistry (1978) 17, 3071.

23. Williams, J. and K. Moreton. Biochem. J. (1980) 185, 483.

24a. Baldwin, D.A. and D.M.R. de Sousa. Biochem. Biophys. Res. Commun. (1981) 99, 1101.

24b. Baldwin, D.A. Biochem. Biophys. Acta (1980) 623, 183.

25. Williams, J., N.D. Chasteen, and K. Moreton. Biochem. J. (1982) 201, 527.

26. Baldwin, D.A., D.M.R. de Sousa, and G. Ford. In The Biochemistry and Physiology of Iron (Saltman, P. and J.C. Hegenaur, eds.). Elsevier Biomedical Press, Amsterdam, (1982), pp. 57-65.

27. Pollack, S., P. Aisen, F.D. Lasky, and G. Vanderhoff. Brit. J. Haematol. (1976) 34, 231.

28. Morgan, E.H. Biochim. Biophys. Acta (1976) 580, 312.

29. Cowart, R.E., N. Kojima, and G.W. Bates. J. Biol. Chem. (1982) 257, 7560.

30. Price, E.M. and J. Gibson. J. Biol. Chem. (1972) 247, 80.

31. Cannon, J.C. and N.D. Chasteen. Biochemistry (1975) 14, 4573.

32a. Folajtar, D.A. and N.D. Chasteen. J. Am. Chem. Soc. (1982) 104, 5775.

32b. Folajtar, D.A. and N.D. Chasteen. In The Biochemistry and Physiology of Iron (Saltman, P. and J. Hegenaur, eds.). Elsevier Biomedical Press, Amsterdam (1982), pp. 35-42.

33. Chasteen, N.D. Trends Biochem. Sci. (1983) 8, 272.

34. Carver, F.J. and E. Frieden. Biochemistry (1978) 17, 169.

35. Krysteva, M.A., J. Mazurier, G. Spik, and J. Montreuil. FEBS Letters (1975) 56, 337.

36. Melchior, W.B. and D. Fahrney. Biochemistry (1970) 9, 251.

37. Folajtar, D.A. A Study of the Thermodynamics of Anion Binding to Human Serum Transferrin. Ph.D. Thesis, University of New Hampshire, Durham, NH. (1982).

38. Ovadi, J., S. Liubor, and P. Elodi. Acta Biochem. Biophys. Acad. Sci. Hung. (1967) 2, 455.

39. Tsou, Chen-Lu. Sci. Sin. (1962) 11, 1535.

40. Roosemont, J.L. Anal. Biochem. (1978) 88, 314.

41. Morgan, E.H. Biochem. Biophys. Acta (1979) 80, 312.

42. Octave, J.N., Y.J. Schneider, A. Trouvet, and R.R. Crichton. Trends Biochem. Sci. (1983) 8, 217.

43. Rao, K., J. van Renswourde, C. Kemptf, and R.D. Klausner. FEBS Letters (1983) 160, 213.

44. Markley, J.L. Acc. Chem. Res. (1975) 8, 70.

45. Butler, J.N. Ionic Equilibrium. A Mathematical Approach. Addison-Wesley, Reading, PA, p. 209.

46. Mazurier, J., M.H. Metz-Boutique, J. Jolles, G. Spik, and P. Jolles. Experientia (1983) 39, 135.

47. Chasteen, N.D., C.P. Thompson, and D.M. Martin. Second International Conference on Bioinorganic Chemistry (1985); Algarus, Portugal, April 14.

48. Means, G.E. and R.E. Feeney. Chemical Modification of Proteins, (1971), Holden-Day, Inc., Cambridge.

49. Habeeb, A.F.S.A. Anal. Biochem. (1966) 14, 328.

50. Chasteen, N.D. and J. Williams. Biochem. J. (1981) 193, 717.

51. Scullane, M.J., L.K. White, and N.D. Chasteen. J. Magn. Reson. (1982) 47, 383.

52. Geoghegan, K.F., J.L. Dallas, and R.E. Feeney. J. Biol. Chem. (1980) 255, 11429.

53. Fraenkel-Conrat, H. Methods Enzymol. (1957) 4, 247.

54. Bezkorovainy, A. and D. Grohlich. Biochim. Biophys. Acta (1970) 214, 37.

58. Goucher, C.R. and J.F. Fuller. J. Biol. Chem. (1964) 239, 2251.

59. Sandell, E.B. Colorimetric Determination of Traces of Metals (1959). Interscience Inc., 524.

60. Bates, G., J. Hegenauer, J. Renner, and P. Saltman. Bioinorg. Chem. (1973) 3, 311.

61. Terron, A. and V. Moreno. Inorg. Chim. Acta (1983) 80, 213.

62. Brown, F.F., I.D. Campbell, R. Henson, C.W.J. Hirst, and R.E. Richards. Eur. J. Biochem. (1973) 38, 54.

63. Karlik, S.J., G.A. Elgavish, and G.L. Eichorn. J. Am. Chem. Soc. (1983) 105, 603.

64. Sakvrai, H., T. Goda, and S. Shimomura. Biochem. Biophys. Res. Commun. (1982), 108, 474.

65. Kalckar, J. J. Biol. Chem. (1947) 167, 445.

66. Spiro, T.G. and P. Saltman. Struct. Bond. (1969) 6, 117.

67. Harrison, P.G. and M.A. Healy. Inorg. Chim. Acta (1983) 80, 279.

68. Theil, E.C. In Advances in Inorganic Biochemistry (Theil, E.C., G.L. Eichorn, and L.G. Marzilli, eds.). Elsevier, NY, Vol. 5 (1983), pp. 1-38.

APPENDIX

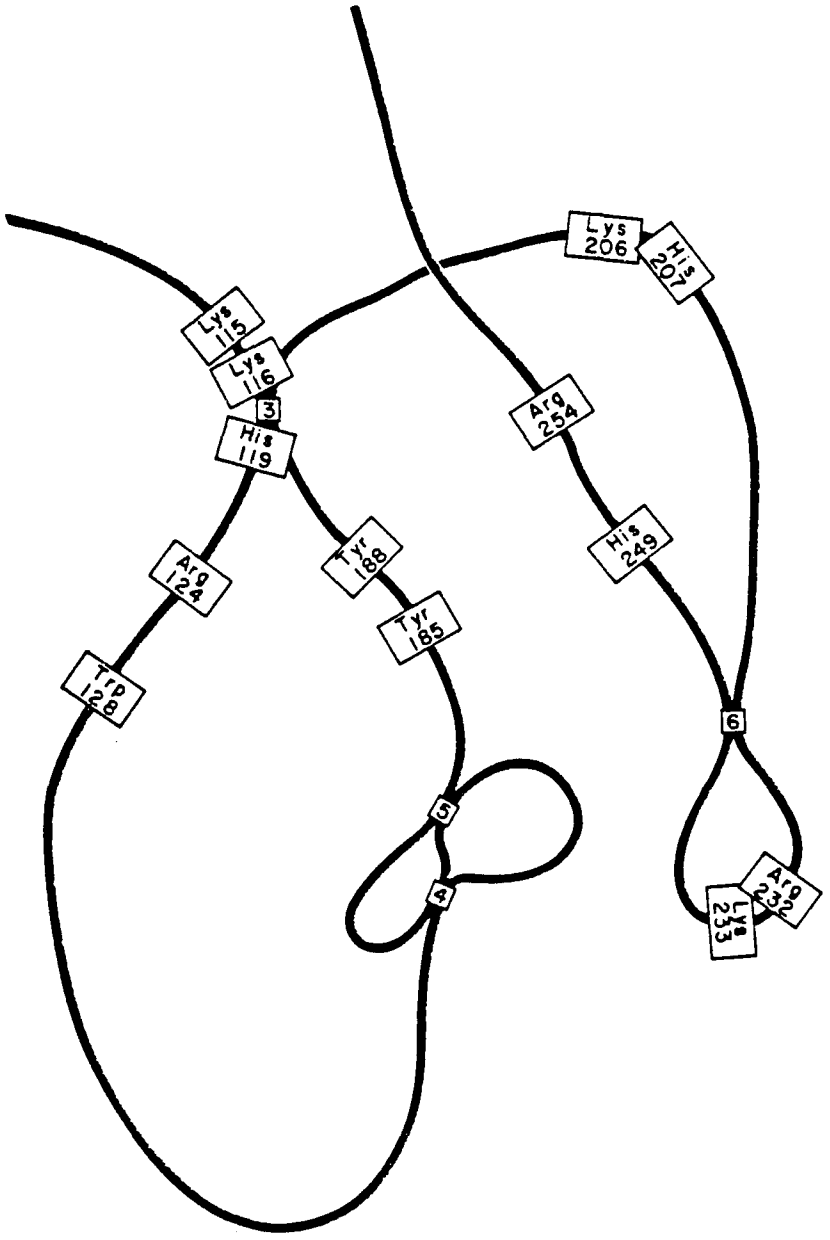

Proposed iron and anion binding peptide of the N-terminal domain in human serum transferrin. (Reprinted with permission from Chasteen, ref. 33.)